The impact of early reflections on binaural cues

Boris Gourévitch[a)] and Romain Brette[b)]
Equipe Audition, Département d' Etudes Cognitives, Ecole Normale Supérieure, 29, rue d' Ulm, 75005 Paris, France

(Received 14 June 2011; revised 16 May 2012; accepted 16 May 2012)

Animals live in cluttered auditory environments, where sounds arrive at the two ears through several paths. Reflections make sound localization difficult, and it is thought that the auditory system deals with this issue by isolating the first wavefront and suppressing later signals. However, in many situations, reflections arrive too early to be suppressed, for example, reflections from the ground in small animals. This paper examines the implications of these early reflections on binaural cues to sound localization, using realistic models of reflecting surfaces and a spherical model of diffraction by the head. The fusion of direct and reflected signals at each ear results in interference patterns in binaural cues as a function of frequency. These cues are maximally modified at frequencies related to the delay between direct and reflected signals, and therefore to the spatial location of the sound source. Thus, natural binaural cues differ from anechoic cues. In particular, the range of interaural time differences is substantially larger than in anechoic environments. Reflections may potentially contribute binaural cues to distance and polar angle when the properties of the reflecting surface are known and stable, for example, for reflections on the ground.
 [http://dx.doi.org/10.1121/1.4726052]

PACS number(s): 43.20.El, 43.66.Pn, 43.66.Qp [MAA] Pages: 9–27

I. INTRODUCTION

To localize sound sources, many species, including humans, rely on subtle differences in the signals arriving at the two ears. The ear closer to the source receives the sound earlier and with a higher level than the other ear. These interaural time differences (ITDs) and interaural level differences (ILDs) are produced by sound propagation and diffraction of sounds by the head, pinnae, and body. They vary systematically with the location of the sound source. The relationship between these binaural cues and sound location have been described in many species, mainly using acoustical measurements of head-related transfer functions (HRTFs) in anechoic chambers, in order to minimize the disturbances due to reflections. However, the acoustical environments animals live in contain many objects that produce reflections, such as trees, natural or artificial walls, and the ground. Even in the open air, with no obstacle, at least one reflection is produced by the ground, and its texture can be very variable, e.g. grass, snow, soil, or asphalt. In principle, these reflections can affect binaural cues, as pointed out by McFadden (1973).

Nevertheless, humans can maintain good localization and segregation abilities in echoic environments (Blauert, 1997; Freyman *et al.*, 2001; Litovsky *et al.*, 1999; Zurek, 1987). This robustness to reflections is thought to be mediated by the *precedence effect* (Litovsky *et al.*, 1999). When a sound and a reflection are separated by less than 1 ms, a fused sound is perceived, with an intermediate localization (*summing localization*). When the delay to the reflection is between about 1 and 5 ms, the perceived source location is dominated by the location of the leading sound - this property is called the "law of the first wavefront" (Blauert, 1997; Shinn-Cunningham *et al.*, 1993; Wallach *et al.*, 1949). When the delay is longer than about 5–10 ms, the two sounds become separately audible (*breakdown of fusion*) and their two distinct localizations are perceived. Note that the breakdown of fusion is longer (~50 ms) for speech or music than for transient sounds (Litovsky *et al.*, 1999; Lochner and Burger, 1964).

Similar findings have been reported in a number of species, with delays in the same range: cats (Cranford, 1982; Populin and Yin, 1998), rats (Kelly, 1974), crickets (Wyttenbach and Hoy, 1993), owls (Keller and Takahashi, 1996a; Spitzer and Takahashi, 2006), and birds (Dent and Dooling, 2004). For example, in cats, localization performance degrades for delays below 0.5 ms, which is consistent with summing localization (Cranford, 1982; Populin and Yin, 1998; Tollin and Yin, 2003). Neural correlates of the precedence effect have also been seen in recordings in the inferior colliculus and auditory cortex of cats: for example, with clicks separated by more than 2 ms, neural responses to the lagging click are suppressed (Dent *et al.*, 2009; Mickey and Middlebrooks, 2001; Yin, 1994).

Thus, many reflections are either suppressed or separately processed by the auditory system. However, not all reflections can be suppressed by the auditory system. Consider the situation illustrated in Fig. 1. The animal faces a sound source, with its ears at a distance p from the ground. Two signals arrive at the animal: the direct sound and its reflection at the ground. Since the shortest path between two points is a straight line, the path length of the reflection can be no more than the distance from the sound source plus $2p$ (see Fig. 1). Thus, the time delay of the reflection is always

[a)]Current address: Centre de Neurosciences Paris-Sud (CNPS), UMR CNRS 8195, Université Paris-Sud, Bâtiment 446, rue Claude Bernard, 91405 Orsay Cedex, France.
[b)]Author to whom correspondence should be addressed. Also at: Laboratoire Psychologie de la Perception, CNRS, Université Paris Descartes, 45, rue des Saints-Pères 75006 Paris, France. Electronic mail : romain.brette@ens.fr

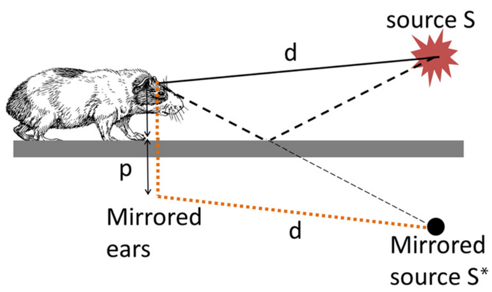

FIG. 1. (Color online) The maximum difference in path length between the direct and reflected sound. The source is at distance d from the ears, which are at height p from the ground. The direct path length is d (solid black line), and the reflected path (dashed black line) is shorter than the dotted path, which has length $d+2p$. Thus, the difference in path length is always smaller than $2p$.

shorter than $2p/c$, where $c \approx 343$ m/s is the speed of sound in air at 20 °C. For example, for a guinea pig, which is about 8 cm tall, this delay is always shorter than 250 μs for all sounds produced on the horizontal plane. This is well within the range when the two sounds are perceptually fused. Therefore, the binaural cues that are available to the animal should be heavily affected by reflections. This hypothesis is supported by real recordings of ILDs in gerbils after reflection by a plywood floor, which show interference patterns (Maki *et al.*, 2003).

In this paper, we first examine early reflections in simple geometrical models to understand how likely they are to produce reflected waves within the "fusion" range for several species (Sec. II). We then examine the impact of these reflections on binaural cues, first when diffraction is absent (Sec. III A), and then using a spherical head model with realistic models of natural textures (Sec. III B). We find that ILDs are more modified than ITDs, and that the variation in ITD can be systematically related to the distance and polar angle from the source (Sec. IV), potentially providing a localization cue. We also notice that variations of ITDs and ILDs due to reflections substantially extend the range of binaural cues that the auditory system has to manage (Sec. V). Finally, we discuss the implications of these results for neural coding of sound location, binaural localization cues, and psychophysical experiments.

II. EARLY REFLECTIONS AND THE PRECEDENCE EFFECT

We consider two simple situations describing the proximity of a human or an animal to the ground or to a wall (Fig. 2). Let S be a sound source at distance d from the head. In the spherical coordinate system typically used in localization studies, S has a lateral angle (azimuth) φ_S and a polar angle (elevation, latitude) θ_S relative to the center of the head (see Appendix A for all symbols). When the sound wave propagating from S encounters an obstacle such as the ground [Fig. 2(A)] or a wall [Fig. 2(B)], it is partly reflected and partly absorbed. The incidence angle of the reflected sound wave is that of a source S* which "mirrors" S relative to the obstacle. As a consequence, for a reflection at the ground, the reflected and direct sound waves have the same lateral angle; for a reflection at a vertical wall, they have the same polar angle.

In the case of a reflection at the ground, the path length d* of the reflection is, at most, the distance of the sound source d plus $2p$ (see Fig. 1). Therefore the delay of the reflected sound is no more than $2p/c$. This upper bound corresponds to the case when the source is directly above the head (i.e., polar angle = 90°), but in many natural situations, this delay is shorter, in particular if the source is far from the ears or close to the ground. This is illustrated in Fig. 3, which shows the computed delay between direct and reflected sounds as a function of the distance from the source to head and the polar or lateral angle of the sound source to the head (see Appendix B for the calculations). For the situation of a zero polar angle, when the source is farther than 10 m then this delay is less than 0.15 ms for animals smaller than cats [Fig. 3(B)], and less than 1 ms for humans [Fig. 3(A)]. The same reasoning applies to a reflection from a wall, where the distance to the ground is replaced by the distance to the wall.

More generally, consider a source and a receiver at distance d from each other. The set of reflection points such

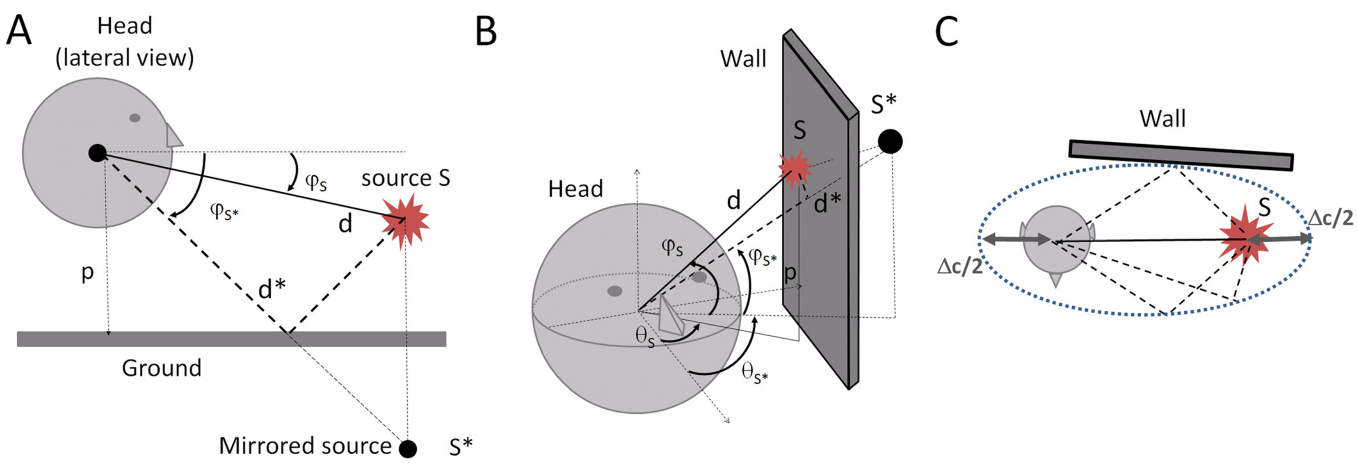

FIG. 2. (Color online) Geometrical models of reflections. Panels A and B show two basic models of sound reflections by the ground and a wall. The polar angle (A) or lateral angle (B) of the sound source is φ_S (A) or θ_S (B) and that of the reflected sound is φ_{S^*} (A) or θ_{S_*} (B): p is the distance between the ears and the obstacle. d* is the reflected path length. Panel C shows, for fixed locations of the source and receiver, that the set of reflection points on the horizontal plane that produce a fixed delay $\Delta = (d^* - d)/c$ forms an ellipse with foci at the source and receiver.

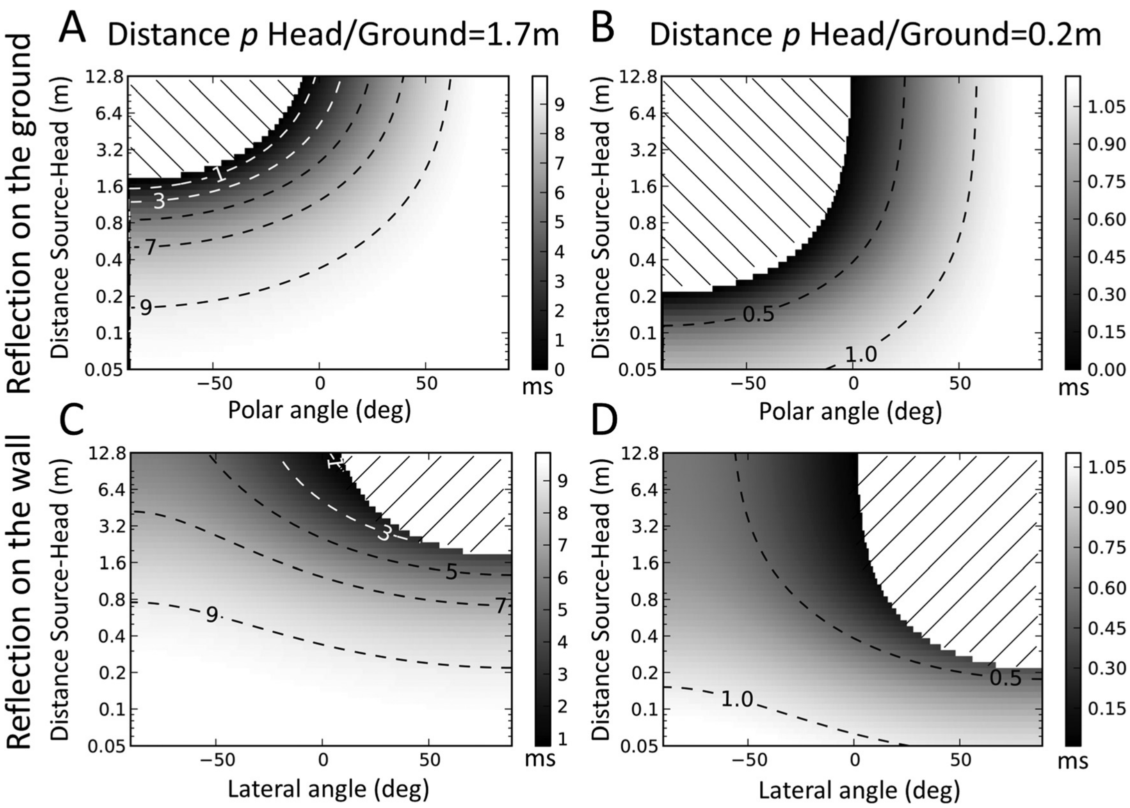

FIG. 3. The computed delay in milliseconds between the direct and the ground-reflected (panels A, B) or wall-reflected (panels C, D) sound waves as a function of the distance from the head and polar angle (A, B) or lateral angle (C, D) of the source. The ground is assumed to be at a distance of $p = 1.7$ m (A) or $p = 0.2$ m (B) from the head. The hatched area represents the geometrically impossible cases where the source would be below the ground. The contours for different delays are shown as dashed lines.

that reflected path length is a fixed quantity d^* is an ellipse[1] with foci at the source and receiver [Fig. 2(C)]. In three dimensions, this would be an ellipsoid. All obstacles that are tangent to this ellipse produce reflections with delay $\Delta = (d^* - d)/c$. For example, delays shorter than $\Delta = 1$ ms are produced by all objects within an ellipse that pass through the two external points aligned with the source and receiver at distance $\Delta c/2 = 17$ cm from them [Fig. 2(C)].

In Table I, we have listed the maximum delay for a reflection at the ground for various different species as well as the values of the delays when the source is 1.5 m away from the ears. For a human, for whom the average distance between ears and ground is 1.7 m, the reflected waves are often delayed by several milliseconds [for example, it is 6.5 ms at a distance of 1.5 m; Fig. 3(A)]. This is within the range of echo suppression in the precedence effect. But the ears of small mammals such as guinea pigs or gerbils are only a few centimeters away from the ground. For instance, even if the gerbil decides to stand up to view its environment, it is only 12 cm high in this fully erect posture, which means a maximum delay of 730 μs for a reflection at the ground. This upper bound corresponds to the situation where the source is at a polar angle of 90°, but when the source is at a polar angle of 0°, i.e. at the same height as the animal, the delay is generally much shorter because the sound hits the ground with grazing incidence. This makes the reflected path length very close to the direct path length geometrically. For example, the delay is only 56 μs for a source at

TABLE I. The computed time delay between the front and reflected sound waves using a ground reflection model for typical ear-ground distances in several species (top line), and for two different source-ground distances (equivalently, two different polar angles).

Species		Human	Dog (Labrador)	Dog (Bulldog)	Cat/ Marmoset	Gerbil	Guinea Pig	Mouse
Ear-ground distance (m)		1.70 (at most)	0.75	0.4	0.2	0.12	0.08	0.02
Front-reflected wave delay (ms)	Maximum delay (ms)	10.3	4.5	2.4	1.2	0.73	0.48	0.12
	dist.: 1.5 m elev.: 0° (source height = ear-ground distance)	6.5	1.82	0.58	0.154	0.056	0.025	0.0016
	dist.: 1.5 m source height = 1 m (elev. in brackets)	4.62 (−25°)	2.3 (9°)	1.3 (22°)	0.66 (28°)	0.39 (30°)	0.26 (32°)	0.07 (33°)

1.5 m from the gerbil. In addition, because they are small, these mammals often move with their ears close to reflecting surfaces, such as embankment slopes. Even for cats (about 20 cm high), the delays are shorter than 1.2 ms in all configurations, and shorter than 1 ms in most natural cases [Fig. 3(B), white line]. Even if the fusion threshold were lower for small mammals than for humans, short delays such as 56 μs are very likely to fall below their fusion threshold. Therefore, the precedence effect cannot account for the processing of early reflections in ecological situations for small mammals. Instead, the binaural cues that are available to these animals should include the impact of early reflections. For this reason, we now focus on small mammals, but we shall come back to the case of humans in the discussion.

III. IMPACT OF REFLECTIONS ON BINAURAL CUES

A. A simple case: Rigid surface and no diffraction

We start by considering an elementary situation with a reflection at a rigid surface but no diffraction effects by the head or similar obstacle. We also neglect the attenuating effect of distance. Our treatment is similar to Sec. 3.1 in Blauert, 1997 ("phasor diagrams" in Fig. 3.8), which also includes a few relevant references such as Leakey (1959) and Wendt (1963). Suppose the source signal is a pure tone with frequency *f*, which we represent as a complex signal $e^{2\pi ift}$. The ear receives the sum of the direct sound (delay δ) and reflected sound (delay $\delta*$):

$$S(t) = e^{2\pi if(t-\delta)} + e^{2\pi if(t-\delta^*)}, \tag{1}$$

which is proportional to $(1+e^{2\pi if\Delta})$, where $\Delta = \delta* - \delta$ is the delay of the reflection to the direct sound. This results in an interference which may be constructive ($f\Delta = n$, n being an integer) or destructive ($f\Delta = n+1/2$) [see Fig. 4(A)]. More precisely, for a fixed delay Δ, the level and phase of the summed signal are periodic functions of the tone frequency *f*, with spectral period $1/\Delta$. At the frequency of each destructive interference [$f = 1/(2\Delta) + n/\Delta$], the level drops to 0 (i.e., $-\infty$ dB), but more interestingly the phase abruptly shifts from $\pi/2$ to $-\pi/2$ [see Fig. 4(B)]. This corresponds to a sign change in the summed vector near the interference frequency.[2]

We now examine the impact of monaural interferences on binaural cues. In the case of a vertical wall, the delay between the direct and reflected sounds is not the same at the two ears [see Fig. 4(C)]. The signal at the left ear is proportional to

$$S_L(t) \propto (1 + e^{2\pi if\Delta_L}) \tag{2}$$

and the signal at the right ear is proportional to

$$S_R(t) \propto (1 + e^{2\pi if\Delta_R})e^{2\pi if\,ITD}. \tag{3}$$

Thus, to understand the consequences on binaural cues, we need to compare the vectors $(1+e^{2\pi if\Delta L})$ and $(1+e^{2\pi if\Delta R})$ [see Fig. 4(D)]. Assuming that the two delays are similar (i.e., $\Delta_L \approx \Delta_R$), the interaural phase difference (IPD) and the ILD are approximately periodic functions of *f*, with

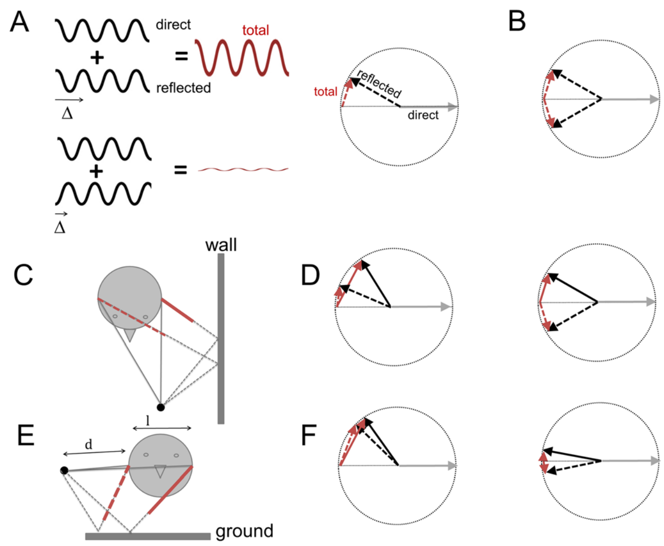

FIG. 4. (Color online) The effect of a reflection on binaural cues in a simple case: An acoustically transparent head. Panel A shows that, for a pure tone of frequency *f*, the interference between the direct and reflected sound is constructive when the delay is $\Delta = n/f$ (top), and destructive when $\Delta = n/f + 1/2$ (bottom). The two signals can be represented as unit vectors on a circle (right), where the angle represents the phase of the reflected sound (dashed black line, "reflected") relative to the direct sound (solid gray arrow). The total signal is the vector sum (dashed line, "total"). Its angle is therefore the phase of the total signal and its length is its amplitude. A short arrow would correspond to a destructive interference. When the phase of the reflected sound goes beyond π (panel B), the phase of the total signal jumps from $\pi/2$ to $-\pi/2$ (panel B). With a reflection at a wall (panel C), the delay between direct and reflected sounds at the left ear (solid arrow) is different from that at the right ear (dashed arrow). Thus, in panel D, the phase of the reflected sound for the left and right ears, relative to the direct sounds, are represented by distinct solid and dashed black arrows, respectively (left). The IPD *change* due to the reflection is the angle between the two summed vectors. It changes discontinuously when the phase of one monaural signal exceeds π (right). With a reflection at the ground (panel E), the delays between reflected and direct sounds are similar but not exactly equal at the left and right ear (solid and dashed thick lines, respectively). Panel F shows that the IPD change due to the reflection is generally small (left), except when a discontinuity occurs, when the phase of one monaural signal exceeds π (right).

spectral period $\Delta \approx (\Delta_L + \Delta_R)/2$. As in the monaural case, two things occur at the frequencies of destructive interferences ($f = 1/(2\Delta_L) + n/\Delta_L$ and $f = 1/(2\Delta_R) + n/\Delta_R$): the ILD goes to $\pm\infty$, and the IPD changes discontinuously. Between the interference frequencies, the IPD change due to the interferences is close to π. Thus, interferences cause large variations in ILD and discontinuities in IPD.

In the case of a reflection at the ground, the delays Δ_L and Δ_R are also slightly different. For example, consider a sound source at polar angle 0° and lateral angle 90° [see Fig. 4(E)]. If d is the distance between the sound to the left ear and l is the interaural distance, then $\Delta_R = \Delta_L(d+l)/d$. This is a small difference, except for very close sources, and therefore the IPD and ILD should not be very degraded in general. However, interferences are still present and cause large changes in ILD and discontinuities in IPD near $f = 1/(2\Delta) + n/\Delta$, as for a reflection at the wall [see Fig. 4(F)]. In particular, the IPD changes by π near interference frequencies.

Thus in this simple situation, we predict that with a reflection the change in IPD and ILD should be a periodic function of frequency with spectral period $1/\Delta$, with maximal changes at the frequencies of destructive interferences: $f = 1/(2\Delta) + n/\Delta$. We now consider more realistic models of the auditory environment.

B. Natural surfaces and diffraction effects

1. Natural surfaces

An incident wave on a real surface is partly reflected and partly absorbed in a way that depends on incidence and frequency. We describe reflections at the ground (the equations are equivalent for a vertical wall if polar angle φ_* is replaced by the lateral angle θ_*). As before, we assume that the receiver is at distance d from the source and at distance d^* from the mirrored source, and we assume that the sound wave is an isotropic spherical wave propagating outward from a central point. The most widely used approach to match the boundary conditions for such a wavefront impinging on a plane finite-impedance surface is the Weyl–Van der Pol solution (Sutherland and Daigle, 1998), where the sound field at the receiver can be expressed as the sum of direct and reflected sound fields. If we define $P(d, f)$ as the complex pressure amplitude at frequency f and distance d from the source (in the absence of reflecting surfaces), then the sound field P^{rec} at the receiver is well approximated by the equation

$$P^{\text{rec}} = P(d,f) + Q(d^*,f,\varphi_{S^*}) \times P(d^*,f), \tag{4}$$

where Q is a spherical reflection factor, a complex-valued function of frequency, angle and distance. The reflected sound field $Q(d^*,f,\varphi_{S^*}) \times P(d^*,f)$ depends on the polar angle φ_{S^*}, the distance d^* (because of the spherical wave hypothesis) and the acoustic properties of the two media (air and ground), which are frequency dependent. Detailed formulae can be found in Appendix C. Many models have been used to describe these acoustic properties for typical outdoor surfaces. We used the Delany–Bazley model (Delany and Bazley, 1970; Miki, 1990), where these properties are described with a single parameter, the effective flow resistivity σ. In Appendix C, we list typical values for a number of natural textures (from Cox and D'Antonio, 2009): high values correspond to rigid surfaces (e.g., concrete) while low values correspond to soft textures (e.g., snow).

Figure 5(A) illustrates the general properties of reflections on natural surfaces. When the ground is soft, a low frequency wave can partially penetrate the surface, which delays the reflected wave. At higher frequencies, the incident sound is partly absorbed and the delay is shorter. The absorption and delay effects are reduced for more rigid surfaces, i.e., those with a higher resistivity σ. With a grazing incidence, the reflection is greater and the delay is longer. These properties are also shown in Figs. 5(B) and 5(C) for two incidence angles and two natural grounds: grass ($\sigma = 10^5$ Pa s m^{-2}) and sand ($\sigma = 6 \times 10^5$ Pa s m^{-2}).

As in the simple situation described in Sec. III A, the direct and reflected waves interfere and produce large variations in level as a function of frequency [see Fig. 6(A)]. Quantitatively, these are not as large as with a rigid surface because the reflections are partly absorbed. Let us first consider a realistic reflecting surface with reflection factor $Q(f)$ and neglect diffraction effects. The pressure decreases with distance as $1/d$. Thus the total pressure at the ear for a pure tone at frequency f is proportional to

$$P^{\text{rec}}(d,f) = \frac{1}{d} + \frac{Q(f)}{d^*} e^{2\pi i f \Delta} = \frac{1}{d} + \frac{|Q(f)|}{d^*} e^{2\pi i f (\Delta + \tau(f))}, \tag{5}$$

where $\tau(f)$ is the phase delay, in seconds, of $Q(f)$. Thus, level and phase vary approximately periodically with frequency,

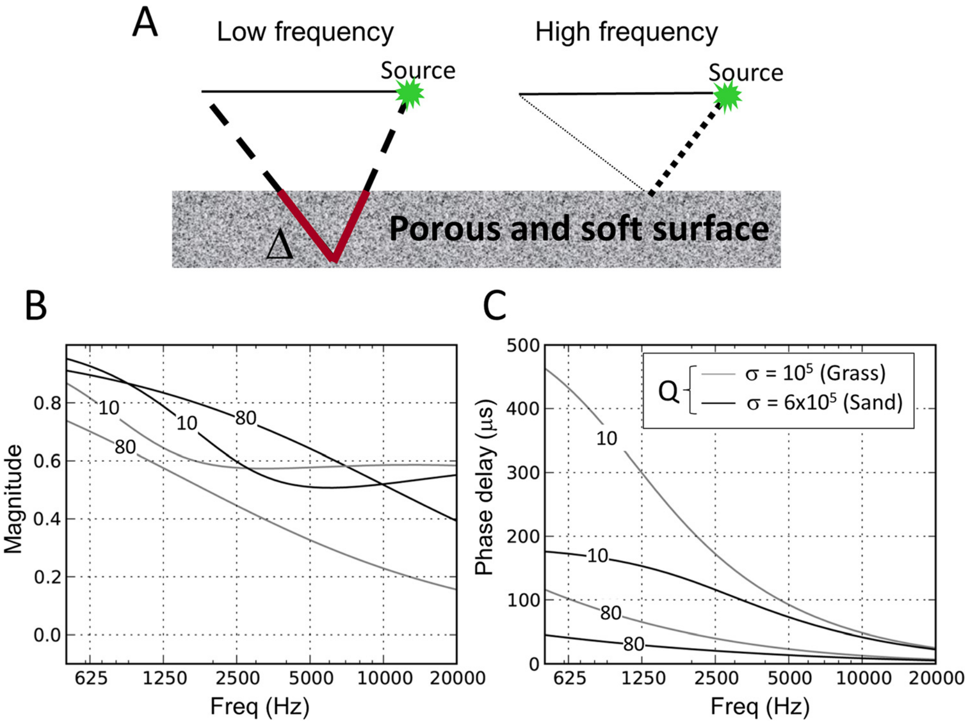

FIG. 5. (Color online) The acoustical properties of natural surfaces. Panel A shows that low frequencies penetrate a porous surface deeper than high frequencies, which produces a delay Δ in the reflected sound. Panel B and C show the amplitude and phase delay of Q, respectively, as a function of frequency (for a sine tone) and for two values of flow resistivity σ. Two incidence polar angles are used (10°, 80°) and are indicated on each curve. The distance between source and receiver is assumed to be $d = 1.5$ m.

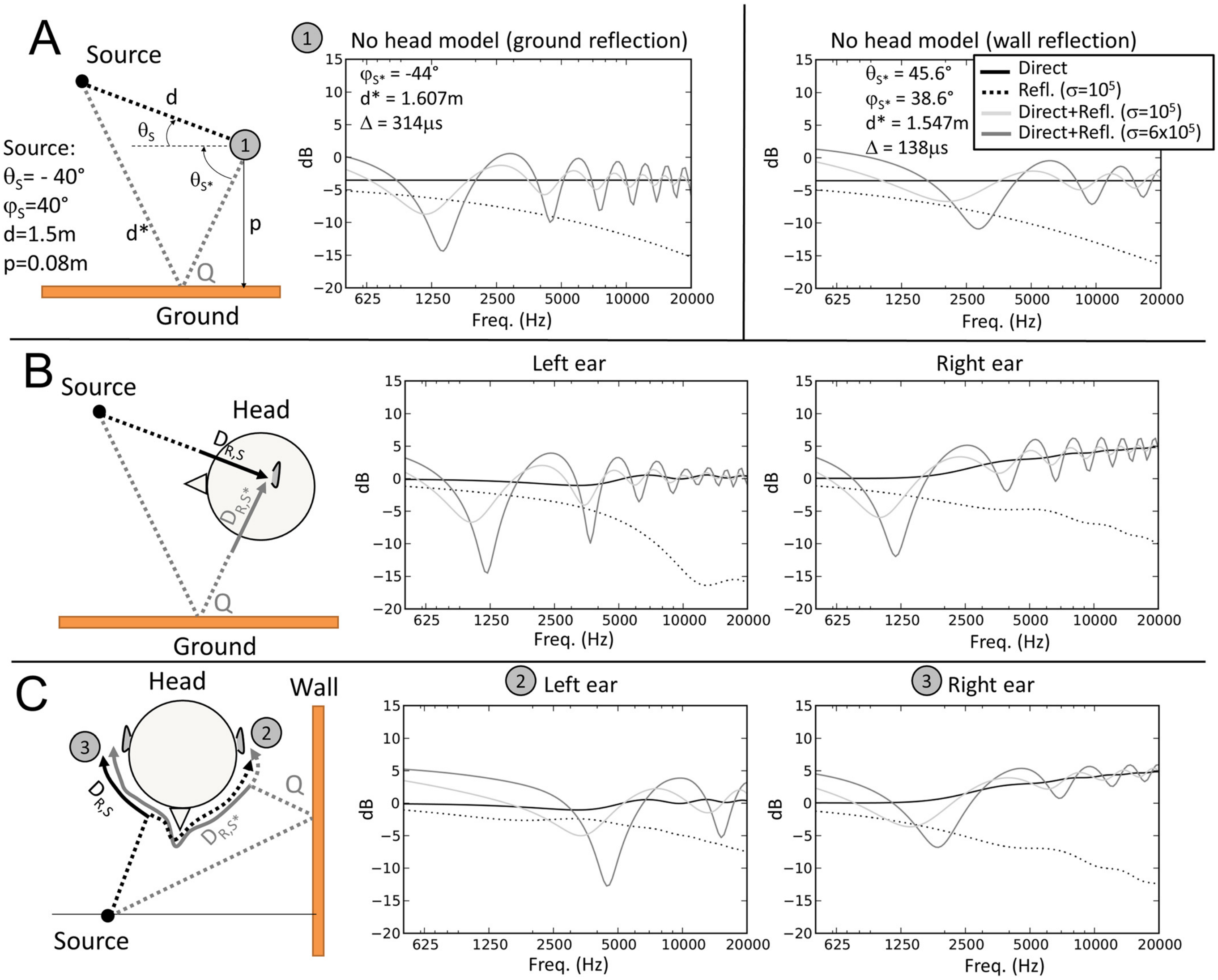

FIG. 6. (Color online) The pressure after a reflection by a ground or a wall for a point source. Panel A shows the pressure at the receiver if there were no head and therefore no diffraction. The geometrical parameters of the source following the conventions of Fig. 1 are indicated at the top left. The parameters of the ground- or wall-reflected wave are shown within the plots. Panels B and C show the pressure at the left and right ears after filtering by the HRTFs of the sphere model, for the ground (B) and wall (C) reflection models. The geometrical parameters of the source are the same as in (A).

with spectral period $\approx 1/\Delta$. The reflection factor $Q(f)$ varies somewhat with frequency, and determines the spectral envelope in Fig. 6(A). The relative amplitude of the interference pattern varies between

$$\frac{1}{d}\left(1-\frac{d}{d^*}|Q|\right) \quad (6)$$

and

$$\frac{1}{d}\left(1+\frac{d}{d^*}|Q|\right) \quad (7)$$

with a first minimum at frequency $f_0 = 1/(2(\Delta+\tau(f_0)))$. For a hard surface, this is close to $f_0 = 1/(2\Delta)$.

In Table II, we report the simple estimates $f_0 = 1/(2\Delta)$ for the first interference frequency and $f_p = 1/\Delta$ for the spectral period, and compare them to the accurate values derived from Eq. (5), for a rigid surface (i.e., $\sigma = \infty$). It can be seen that the simple estimate of the spectral period f_p is very accurate for high σ, while the first interference frequency f_0 seems to be slightly overestimated. These estimates become less accurate as σ decreases, i.e., for more porous surfaces. This is to be expected since porous surfaces introduce an

TABLE II. Computed values found in the spectra shown in Fig. 6(A) and estimates $f_0 = 1/(2\Delta)$ for the first interference frequency and $f_p = 1/\Delta$ for the spectral period (see Secs. III A and III B).

		Ground reflection	Wall reflection
First notch	Computed value $\sigma = 10^5$	1179 Hz	2051 Hz
f_0	Computed value $\sigma = 6.10^5$	1418 Hz	2878 Hz
	Estimate ($\sigma = \infty$)	1590 Hz	3624 Hz
Spectral Period	Computed value $\sigma = 10^5$	3103 Hz	6606 Hz
f_p	Computed value $\sigma = 6.10^5$	3151 Hz	6942 Hz
	Estimate ($\sigma = \infty$)	3180 Hz	7248 Hz

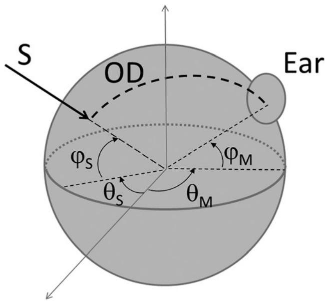

FIG. 7. The orthodromic distance OD between the point of incidence of a source S with the surface of a sphere (incidence angles (θ_S, φ_S)) and the ear (coordinates (θ_M, φ_M)). See Appendix D for the formulas.

additional delay in low frequencies because of the properties of the reflection factor Q (see Fig. 5).

2. Diffraction effects

The second aspect that we must take into account is the diffraction of sounds by the head. This effect is described by head-related transfer functions (HRTFs). The HRTF is the pressure at the ear divided by the reference free-field pressure at the center of the head, for a source at a given location. The head scatters sound waves in a way that depends on the incidence of the wave relative to the head and the sound frequency, and therefore HRTFs are functions of frequency, distance, lateral angle, and polar angle. For a sinetone frequency f, we can thus define HRTFs with reflections using the Weyl–Van der Pol equation described above:

$$H^{\mathrm{rec}}(d,f,(\theta_S,\varphi_S)) = H(d,f,(\theta_S,\varphi_S)) + Q.H(d^*,f,(\theta_{S^*},\varphi_{S^*})). \quad (8)$$

The HTRF for the left and right ears will be denoted H_L and H_R, respectively. In the following calculations, we use a spherical head model with shifted ears, for which the diffraction function is completely known and has been extensively described, for instance, in (Duda and Martens, 1998; Ono *et al.*, 2008). Details are given in Appendix D. The geometrical properties of the spherical head model were chosen to give a match to the shape of a guinea pig head, with ears at the back and top: a head radius of 2 cm and ears at a lateral angle of $\pm 110°$ and a polar angle of $+30°$. The head was assumed to be at $p = 8$ cm from the ground or wall, corresponding to the average distance between ears and ground in guinea pigs.

The results are shown in Figs. 6(B) and 6(C). As can be seen, the monaural interference patterns are qualitatively similar when diffraction effects are introduced. However, these introduce additional delays which must be taken into account in our estimates of f_0 and f_p. Indeed, for the right ear, head filtering introduces a phase shift $\phi_R^S(f) = \arg(H_R(f,d,(\theta_S,\varphi_S)))$ for the direct wave and $\phi_R^{S*}(f) = \arg(H_R(f,d^*,(\theta_{S^*},\varphi_{S^*})))$ for the reflected wave. The phase difference $\phi_R^{S*}(f) - \phi_R^S(f)$ adds to the phase of the reflection wave in Eq. (1). Thus, the first minima in the sound spectrum at the right ear should occur at frequency f_0 such that $2\pi f_0\Delta + 2\pi f_0\tau(f_0) + \phi_R^{S*}(f_0) - \phi_R^S(f_0) = \pi$. The phase shift induced by head filtering can be approximated by the time needed by the sound wave to travel around the spherical head from its impact point with the head to the right ear. This distance is called an "orthodromic"[3] distance and is the distance $r\mathrm{OD}(p_1, p_2)$ between two points p_1 and p_2 on a sphere of radius r (Deza and Deza, 2006), see Fig. 7 and Appendix D for details. We can therefore approximate the phase difference $\phi_R^{S*}(f) - \phi_R^S(f)$ as follows:

$$\begin{aligned}\phi_R^{S*}(f) - \phi_R^S(f) &\approx 2\pi f\cdot\frac{r}{c}\cdot(\mathrm{OD}((\theta_{S^*},\varphi_{S^*});(-\theta_M,\varphi_M)) \\ &\quad - \mathrm{OD}((\theta_S,\varphi_S);(-\theta_M,\varphi_M))) \\ &\approx 2\pi f\Delta_{\phi R},\end{aligned} \quad (9)$$

where $\Delta_{\phi R}$ is a propagation delay that does not depend on frequency. This is applicable when the wavelength is small compared to the head size. Thus our estimates of interference parameters for a rigid surface with $\sigma=\infty$ are now

$$f_0 = \frac{1}{2(\Delta + \Delta_{\phi R})} \text{ and } f_p = \frac{1}{\Delta + \Delta_{\phi R}}. \quad (10)$$

Table III shows that the interference spectral period f_p is very well approximated by this formula, while the first interference frequency f_0 is overestimated. Part of the explanation is probably the additional delays in low frequency introduced by diffraction (Kuhn, 1977), which we did not take into account in our formula.

3. Impact on ITDs and ILDs

As is shown in Fig. 8, these monaural interferences result in oscillations in ILD and ITD as a function of frequency. When the sound is reflected on a vertical wall [Figs. 8(A) and 8(B)], the spectral period f_p of interferences is different for the two ears, which has two consequences. First, all spectral notches at each ear are seen in the ILD. For instance, in the example shown in Figs. 8(A) and 8(B) [as well as Fig. 6(A)], because the wall

TABLE III. Computed values derived from Eq. (5) and prediction for the first notch and the interference spectral period frequency [see Eq. (10)].

		Wall reflection		Ground reflection	
		Left ear	Right ear	Left ear	Right ear
First notch	Computed value $\sigma = 10^5$	3357 Hz	1375 Hz	1011 Hz	1011 Hz
f_0	Computed value $\sigma = 6\times10^5$	4428 Hz	1871 Hz	1216 Hz	1179 Hz
	Estimate ($\sigma = \infty$)	6105 Hz	2675 Hz	1352 Hz	1376 Hz
Spectral Period	Computed value $\sigma = 10^5$	10 240 Hz	4876 Hz	2626 Hz	2695 Hz
f_p	Computed value $\sigma = 6\times10^5$	11 378 Hz	5120 Hz	2695 Hz	2768 Hz
	Estimate ($\sigma = \infty$)	12 211 Hz	5351 Hz	2703 Hz	2753 Hz

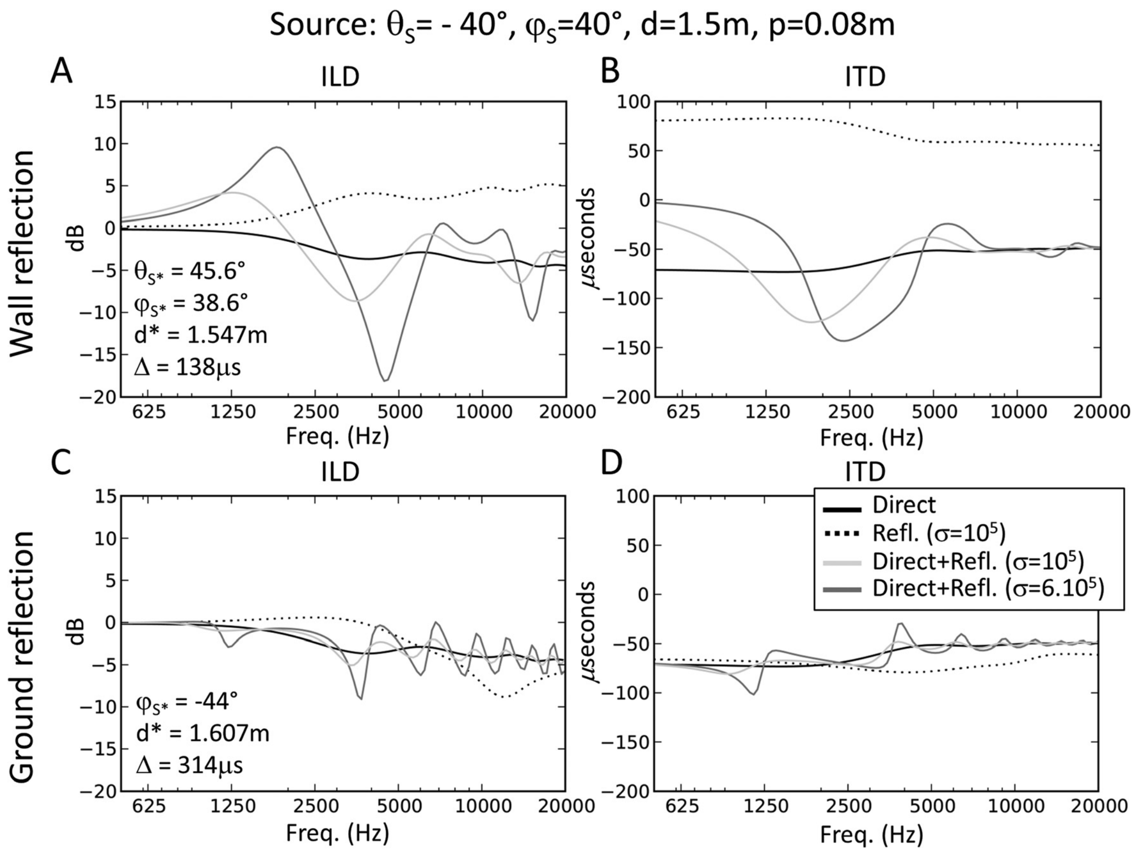

FIG. 8. Panels A and B show the ILD and ITD estimated from HRTFs of the sphere model after reflection by a wall. Panels C and D show these ILD and ITD after reflection by the ground. The parameters of the source following the conventions of Fig. 1 are indicated at the top. The parameters of wall- and ground-reflected waves are shown within plots A and C, respectively.

faces the left ear, the variations of acoustical pressure vs frequency are stronger for the left ear. Thus, the first maximum in ILD [Fig. 8(A)] stems from the right ear (1871 Hz), though the strongest one comes from the left ear (4428 Hz). The two interference spectral periods from each ear are present in the ILD interference pattern—note the irregular oscillatory pattern in Fig. 8(A). Second, the interference patterns for both ILD and ITD are much stronger for the wall reflection than for the ground reflection. Indeed, for a reflection at the ground, the monaural interference patterns are similar for the two ears, with almost identical values across ears for both f_0 and f_p (Table III). This is because the direct and reflected sound have the same lateral angle, so that $\phi_R^{S*}(f) \approx \phi_R^{S}(f)$. As a consequence, the ILD is much less affected than with a reflection at a wall.

With weakly reflective textures such as snow, interferences in ITDs and ILDs are not visible with a ground reflection. They are present, although reduced, with a wall reflection. With strongly reflective textures such as asphalt, the magnitude of interferences is larger compared to the σ values used here.

Monaural spectral notches correspond to dramatic changes in ITD. For this reason, the same interference pattern is expected in the ITD vs frequency curve as in the ILD vs frequency curves. However, while the spectral periodicity of these patterns agree well, the precise frequencies of extrema in ITDs can be more difficult to predict: for a reflection at the ground, monaural interferences are similar in both ears and the abrupt changes in ITDs match the extrema in ILDs [see Fig. 8(D)], but for a reflection at a wall, the destructive interferences may appear at different frequencies at the two ears, and the resulting binaural interference pattern is more complex. In general, the extrema in ITDs and ILDs are interlaced, and extrema in ITDs are closer to extrema in ILDs when the reflecting surface is harder. For instance, in Fig. 8(B), the first peak in ITD is almost in the middle of two ILD extrema for $\sigma = 10^5$ (gray solid line) while it is close to the first peak in ILD for $\sigma = 6 \times 10^5$ (black solid line).

We may wonder whether these interference patterns overlap with the hearing range of various species. In Table IV, we report the computed values $f_0 = 1/(2(\Delta + \Delta_{\phi R}))$ as an estimate for the first extrema in ILD/ITD after ground reflection for the animals in Table I. The interference spectral period f_p would be close to twice these values. This estimate corresponds to an acoustically hard surface—remember that the calculated values will be slightly lower for an acoustically softer surface which introduces an additional delay in low frequencies. For these calculations, ear position and head radius were estimated from photographs, and for simplicity assuming a spherical head (many animals do not have. This has only a limited influence on final values). For tall mammals such as humans, Table IV shows that ITDs and ILDs can be disturbed at low frequencies. However, it could be argued that the law of the first wavefront, which occurs for such delays, will limit this impact by suppressing the reflection. We return to this issue in the discussion. For small mammals (e.g., cats, gerbils, guinea pigs),

TABLE IV. Approximation of spectral period and first extrema frequency of interferences in sound waves incoming at the right ear in a ground reflection model for the various species of Table I. The distance from the source is assumed to be 1.5 m and the same two sets of source height/polar angle as in Table I are used. The lateral angle is assumed to be $-40°$.

Species		Human	Dog (Labrador)	Dog (Bulldog)	Cat	Gerbil	Guinea Pig	Mouse
Head radius (cm)		8.75	8	9	4.5	1.3	2	0.8
Angles θ_M, φ_M (°)		100,−5	110,30	110,30	110,40	110,40	110,30	110,40
Minimum f_0 (Hz) (across all sources considered in Sec. V, Fig. 12)		49	111	208	417	685	1042	4167
dist.: 1.5 m elev.: 0° (source height = ear-ground distance)	First extremum f_0 (Hz)	76	260	761	2831	8352	17 700	253 000
	Interference period f_p (Hz)	152	520	1522	5662	16 700	35 400	506 000
dist.: 1.5 m source height = 1 m	First extremum f_0 (Hz)	107	205	342	659	1182	1685	6045
	Interference period f_p (Hz)	214	410	684	1318	2364	3370	12 000

the interference spectral period f_p is generally large for sources at a polar angle of 0°, unless they are very close, and therefore only the first extremum f_0 is expected to impact sound localization. However, for a fixed source at distance 1.5 m and height 1 m (two last rows), giving a high polar angle for small mammals, both f_0 and f_p fall within the physiologically relevant frequency range for these animals. In this case, interferences in ITD and ILD may impact sound localization. At first sight, it would seem that this impact is negative because it degrades the "normal" binaural cues. However, as is outlined in the next section, if these interferences can be systematically related to the source location, in particular distance, then they may also provide a usable cue for sound localization.

IV. INTERFERENCES AS LOCALIZATION CUES

The interference pattern is determined by the delay between the direct and reflected sounds, which depends on the location of the source. In Fig. 9, we show the computed change in ILD and ITD produced by the reflection (see Appendix E), as a function of frequency and either polar angle or lateral angle, for a reflecting surface with a flow resistivity of 6×10^5 (sand).

The interferences in the ITD vs frequency curves follow the same pattern as in the ILD vs frequency curves. Similar interference patterns as a function of polar angle have been obtained from real recordings of ILDs in gerbils after reflection by a plywood floor (Maki *et al.*, 2003). It can be seen

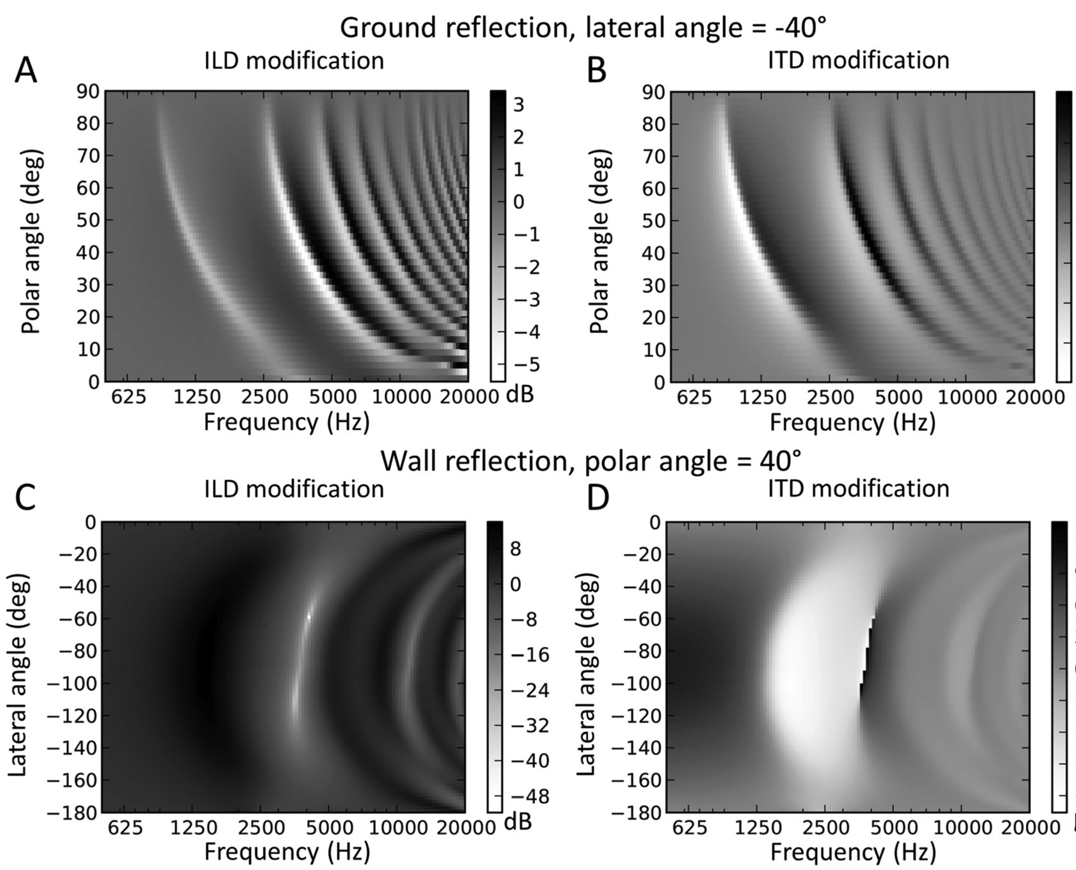

FIG. 9. The ITD and ILD changes produced by a reflection (A,B: ground; C,D: wall). In panels A and B, the lateral angle is set to $-40°$ for the ground reflection, as in Fig. 8. In panels C and D, the polar angle is set to 40° for the wall reflection.

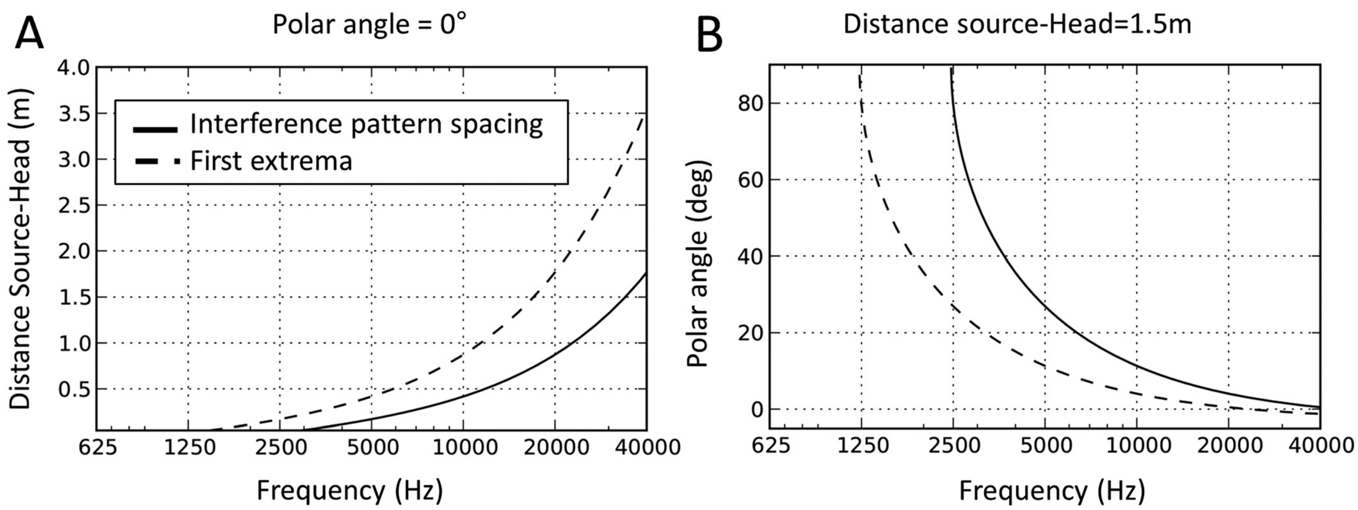

FIG. 10. Panel A shows, for the ground reflection, the relationship between source-head distance (vertical axis) and interference pattern spacing and first extrema (horizontal axis), for a polar angle of 0°. Panel B shows, for the ground reflection, the relationship between polar angle and interference pattern spacing and first extrema, for a source-head distance of 1.5 m. The source is assumed to be at the same level as the animal and its lateral angle is −40°.

that there is a systematic variation in both the first interference frequency f_0 and the interference spectral period f_p with polar angle for ground reflection and lateral angle for wall reflections. These two values might thus be usable as localization cues. However, for a reflection at a wall, they also depend on the location and orientation of the reflecting surface, which are very variable in real environments (see Appendix B). The unpredictable variability in binaural cues may therefore be seen as "noise" but for a reflection at the ground, this variability is predictable, because the ground is generally approximately horizontal and at a fixed distance from the ears. Indeed, if the polar angle is known, then the distance from the source can be estimated from the first interference frequency f_0 or the interference spectral period f_p [Fig. 10(A)]. As we have seen, these two values are not very sensitive to the nature of the ground. Conversely, if the distance is known, then the source polar angle can be estimated [Fig. 10(B)]. Nevertheless, the interference spectral period would probably not be a very helpful localization cue for large distances, because very few interference peaks occur within the physiological frequency region, as the second peak occurs at frequency $f_0 + f_p \approx 3f_0$. However, the first interference frequency would remain useful over a larger distance range.

It is also useful to look at the change of the values of ITD and ILD relative to when there is no reflection. In Fig. 11, we show this relative change for the situation shown in Figs. 6 and 8. It appears that ILD is more affected than ITD, both for ground and wall reflections. Even for the moderate flow resistivity value σ of 6×10^5 used for the calculations in this figure, the variations in ILDs are very large in both cases, especially for low frequencies. Indeed, many surfaces are very reflecting in low frequency and the ILD is very small in the absence of reflections. Both binaural cues are much less affected by the ground than by the wall. Although the position of the ITD and ILD extrema depends on the delay between the direct and reflected sounds and thus may be viewed as information, the amplitude of the changes depends on surface type: the amplitude is higher for more rigid surfaces. In general, then, these may be seen as

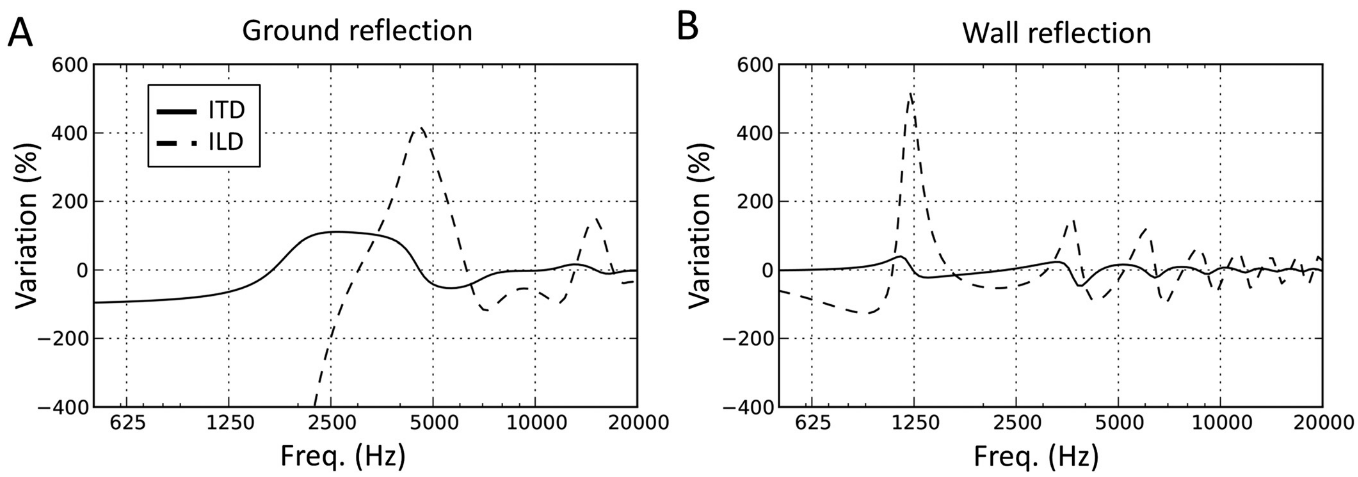

FIG. 11. The relative change in ITD and ILD due to reflections, compared to ITD and ILD of the direct wave, for the source parameters used in Figs. 6 and 10. The sound wave is reflected by (A) the ground or (B) a wall. The flow resistivity is $\sigma = 6 \times 10^5$.

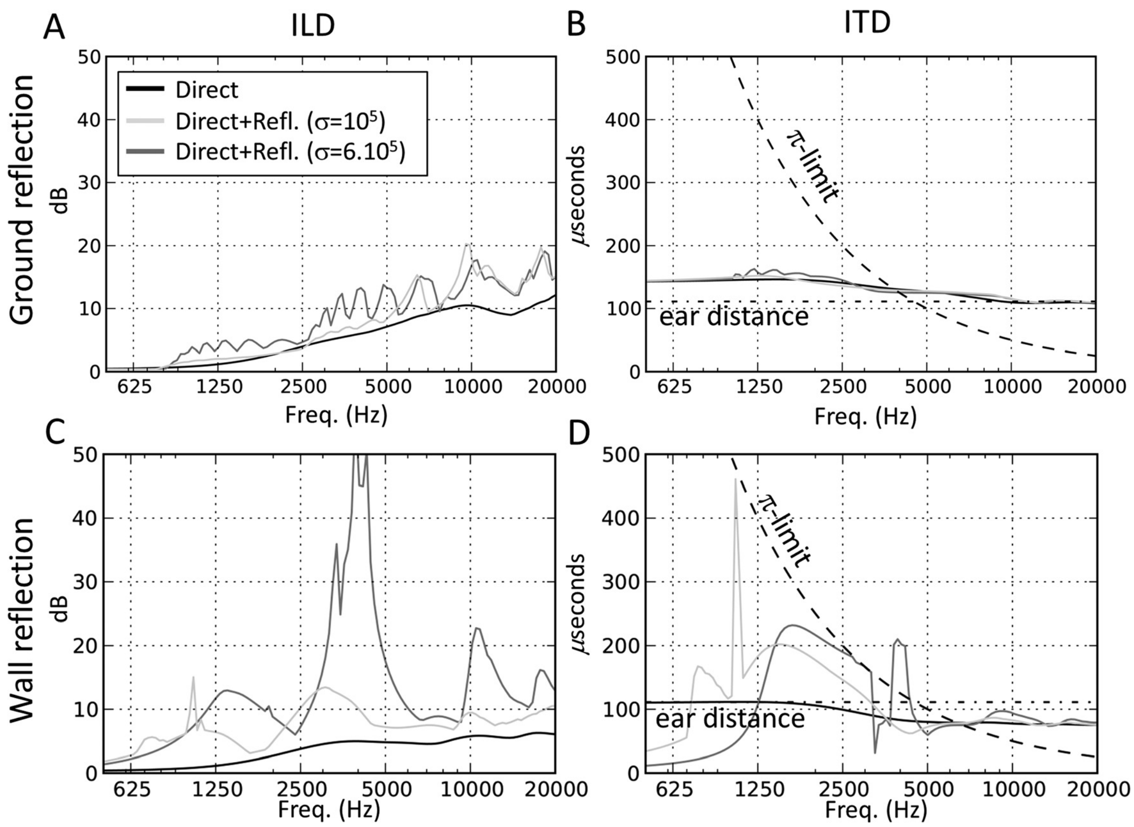

FIG. 12. The panels A and B show the maximum ILD and ITD with and without ground reflections, for sounds between 1 and 20 m from the head and with a ground-head distance of 0.08 m. The panels C and D show these maximum ILD and ITD with and without wall reflections. The π-limit and the ITD corresponding to the distance between the two ears (3.8 cm in the sphere model) are indicated in dashed lines in B and D.

degradation of binaural cues, and it appears that ITD is the more reliable.

V. RANGES OF ITD AND ILD WITH REFLECTIONS

We now look at how reflections change the range of ITDs and ILDs processed by the auditory system. We calculated the maximum ITD and ILD as a function of frequency across lateral angle and polar angle coordinates within a large grid of 393 spherical positions evenly distributed around the sphere (between –45° and 90° polar angle), similar to that in Behrend *et al.* (2004), and for distances between 1 and 20 m at increments of 50 cm. Figure 12 shows the results for ground and wall reflections. In both cases, the range of ILDs is greatly extended, especially in low frequencies where ILDs are usually small. Without reflections, ILDs are always smaller than about 10 dB. With a reflection at a wall, they can reach more than 30 dB. This phenomenon is accentuated by surfaces with higher flow resistivities.

The range of ITDs is not strongly affected by a reflection at the ground, but it is very much extended with wall reflections, as was noted by McFadden (1973). Without reflections, the ITD changes continuously with frequency and therefore it is usually estimated by "unwrapping" the IPD, that is, by considering that ITD is a function of frequency that is consistent with IPD modulo 2π and has minimum variation: $|2\pi f_2 \mathrm{ITD}(f_2) - 2\pi f_1 \mathrm{ITD}(f_1)| < \pi$ for two neighboring frequencies f_1 and f_2. This does not work with reflections because destructive interferences make ITD a discontinuous function of frequency. Therefore, for Fig. 12, we chose a conservative estimate, by choosing the ITD consistent with IPD that is closest to the anechoic ITD (see details in Appendix E). Thus the range of ITDs with reflections shown in Fig. 12 is an underestimation. For high frequencies, this underestimation is not very informative because the method artificially constrains the estimate to be within $1/(2f)$ of the anechoic ITD. This is known as the π-limit (Brand *et al.*, 2002; Hancock and Delgutte, 2004; Joris and Yin, 2007; McAlpine *et al.*, 2001). However, for low frequencies and reflections on a wall, ITDs can be arbitrarily large within this limit, especially for surfaces with high flow resistivities. Indeed, as we have seen, the IPD is close to π near a destructive interference. This means that the range of ITDs is very much extended by reflections at low frequencies compared to an anechoic environment.

VI. DISCUSSION AND SUMMARY

A. Limitations of the models

Although we have tried to consider realistic acoustic properties for the reflecting surfaces, our models rely on a number of approximations.

First, we did not consider the frequency-dependent absorption properties of air (ISO 9613-1:1993, 1993). In particular, high frequencies tend to be more attenuated than lower frequencies and the effect depends on distance. However, as we only considered early reflections, the spectrum of the direct and reflected sounds should be almost identical, and therefore the differential effects of air absorption should be minor.

Second, we only considered a single reflection. In a real environment, there are many more reflections. In addition, under specific atmospheric conditions, a downward refraction by the atmosphere might generate additional ray paths and therefore one or more reflections to the ground (Sutherland and Daigle, 1998). Late reflections are assumed to be suppressed by the auditory system, via the precedence effect, but there may be additional early reflections. However, at least for low frequencies, most of the reflected power should be contributed by large flat and thick surfaces such as the ground. But a natural ground is not a perfectly horizontal surface. In particular, small irregularities such as rock or stones may heavily deviate and attenuate the reflection of high frequency sounds. For instance, an obstacle of less than 5 cm interferes with sound waves above 7 kHz. As a consequence, interferences at such high frequencies might be of lower amplitude in real environments than in our model. We also assumed that the texture is homogeneous and of infinite depth, which is clearly not the case in natural environments. Nonetheless, many studies have shown that field measurements of sound propagation are in close agreement with the theoretical models used in this paper, in particular for grass which has an average flow resistivity similar to the values we used (Chessell, 1977; Embleton *et al.*, 1983; Rasmussen, 1981).

Thirdly, the sphere is a highly simplified model of the head of an animal. We introduced shifted ears but other aspects such as the nose and the torso also play a role in the diffraction of sounds by the body.

Finally, we only considered point sources with omnidirectional directivity (i.e., monopoles). Real sources may deviate from this model, for example human speech or mammal vocalizations are not omnidirectional. For these sources, we would expect that the direct sound has more power than the reflected one.

B. Impact of reflections on binaural cues

For many small animals such as cats and guinea pigs, the ground contributes early reflections with delays no longer than about a millisecond. This maximum delay is only for a sound source near the ears and it quickly decreases with distance: for example, it is just 150 μs for a sound source at 1.5 m from the head of a cat. It is unlikely that such reflections can be suppressed by the auditory system, considering that psychophysical measurements indicate that the threshold for fusion is close to 1 ms. Therefore, the reflection modifies the binaural cues perceived by the animal, and so the perceived binaural cues in an ecological environment, even a simple one with only a ground, are not the same as in an anechoic environment.

In barn owls, a number of studies have addressed the neural and behavioral correlates of acoustical reflections (Keller and Takahashi, 1996a, 1996b, 2005; Nelson and Takahashi, 2010; Spitzer and Takahashi, 2006). In a natural environment, the ground can be far from the owl's ears when it flies, but when it is about to catch its prey the ground is very close. Therefore the same remarks as for small animals apply, and the maximum delay of the reflected sound is a fraction of millisecond. For example, for a mouse just below the owl, the delay is about 100 μs, which corresponds to an interference at frequency 5 kHz, right in the middle of the hearing range of these animals. This is well below the fusion threshold for owls, about 0.5 ms (Keller and Takahashi, 1996a, 1996b). In binaural neurons of the inferior colliculus, the response to a reflection is suppressed when the delay is longer than 0.5 ms, but it is consistent with cross-correlation of the summed direct and reflected signals below 0.5 ms (Keller and Takahashi, 1996b). This suggests that the reflected signal is indeed retained by the auditory system for such short delays. These electrophysiological observations are consistent with behavioral measurements, in which owls turn their head to the leading sound when the delay is longer than 1 ms (Keller and Takahashi, 1996a).

The combination of the direct and reflected sounds leads to monaural interferences, around frequencies $f = 1/(2\Delta) + n/\Delta$, which are then seen in binaural cues. Periodic distortions in ILDs have been previously reported in studies of simulated gerbil HRTFs with ground reflection (Grace *et al.*, 2008) and in human HRTFs with ground reflection (Rakerd and Hartmann, 1985) or for the ear facing a very near wall (Shinn-Cunningham *et al.*, 2005). The largest modifications occur for reflections at a vertical wall, because the lateral angle and therefore the binaural cues are very different for the two sounds. For a reflection at the ground, the modifications are smaller but still very significant near interference frequencies. ILDs are typically more affected than ITDs, because ILDs are defined as a ratio of monaural levels. Indeed, even though a constructive interference cannot produce a gain larger than 6 dB, the change in ILD can reach 10–15 dB because of destructive interferences.

C. Humans vs small animals

We have focused our study on small animals that live on the ground. In these animals, delays between direct and reflected sounds are very short in many situations. For humans, the delays of reflected sounds can be longer, up to 10 ms for a reflection at the ground. It might be argued that this is beyond the fusion threshold and therefore such echoes should be suppressed by the auditory system. However, there are reasons to think that our results may also apply to humans. First, the delays are shorter when the source is far [the delay is < 1 ms when the source is > 15 m away, see Fig. 3(A)], and therefore interferences in binaural cues should be seen for distant sources. Second, even when the delay is long, the processing of binaural cues by the auditory system might still be impacted, because they are processed in frequency bands, where the direct and reflected sounds may interact. The duration of the impulse response of an auditory filter is inversely related to its bandwidth and therefore with its center frequency, and two delayed impulse responses interact if the delay is shorter than a few periods. The first interference occurs at frequency $f = 1/(2\Delta)$: for that frequency, the delay corresponds to only half a period of the waveform. Therefore, this interference should be seen in the response of binaural neurons, at least in the earliest stages of the binaural pathway. This means that, in the responses of these neurons, the direct and reflected sounds should merge when the delay is smaller than a value which is inversely proportional to frequency. This is consistent with psychophysical measurements in humans (Dizon and Colburn, 2006; Kirikae *et al.*, 1971).

Thus it seems plausible that early reflections also interfere with direct sounds in humans and affect binaural cues, so that all the results shown here should also apply to humans. The main difference with small animals is that humans stand, and therefore the ground is further from the ears. This implies that delays between direct and ground reflected sounds are typically longer for sources in the horizontal plane, even at relatively far distances. Longer delays mean lower interference frequencies. For example, with a 10 ms delay, the first interference frequency is 50 Hz and the next ones are at 150 and 250 Hz; with a 6.5 ms delay, i.e., a distance of 1.5 m, they are 77, 231, and 385 Hz. These are in the hearing range of humans. In addition, as we have seen in Sec. III B, natural surfaces are generally very reflecting at low frequencies. Moreover, humans typically stand on artificial textures such as concrete or asphalt that are strongly reflective. Therefore, we expect strong modifications of low frequency binaural cues for sources at the same height as the listener. Finally, we note that, as for owls, the delays are short if the source, instead of the ears of the listener, is close to the ground. In this case, all the results we have shown directly apply.

D. Noise and information contributed by early reflections

The interferences between direct and reflected sounds modify the binaural cues, especially ILDs. These modifications could be seen as a source of noise in the localization of sound sources. The relevant issue is the variability of these cues for a given location, when other unknown factors are allowed to vary, for example the nature of the ground or the exact orientation of the reflecting surface. With this point of view, the changes introduced by walls or similar obstacles would qualify as noise, because they are large and very sensitive to other parameters that seem difficult to precisely estimate by other means, such as the orientation and texture of the obstacle. Indeed, performance in localization is degraded by strong reflections (Croghan and Grantham, 2010; Giguère and Abel, 1993; Rakerd and Hartmann, 2005) and vision is given a stronger perceptual weight (Truax, 1999).

How can the auditory system deal with these disturbances? For broadband sounds, frequency integration might be a useful strategy: ITDs and ILDs vary with respect to frequency around an average value which could be used to estimate the source location, as seen in Fig. 8. In echoic environments, human performance is indeed poor for pure tones (Hartmann, 1983; Rakerd and Hartmann, 1985) and transients seem to be important for localization in rooms (Hartmann and Rakerd, 1989; Rakerd and Hartmann, 1985). Another possible strategy for continuous sounds is to use the motion of the source or the voluntary motion of the head, and to select the most favorable configurations—for example, on the basis of variability of binaural cues across frequency. However, we note that the detectability of a masked signal is not generally improved by its motion (Xiao and Grantham, 1997). A third hypothesis is that the auditory system may select the most "plausible" binaural cue: for example, very large values for ITDs could be seen as implausible and discarded, giving a stronger weight for ILD (Rakerd and Hartmann, 1985). We found that ITDs were generally less affected by reflections than ILDs. This would suggest that the auditory system should rely more on ITDs than on ILDs. However, for high frequencies, ITD is ambiguous unless the sound is broadband. Even though high frequency neurons in the inferior colliculus are sensitive to envelope ITDs (Griffin *et al.*, 2005; Joris, 2003; Nelson and Takahashi, 2010), a recent study of the directional sensitivity of such neurons in reverberation suggests that ILD provides better directional information than envelope ITDs in high frequencies (Devore and Delgutte, 2010).

Binaural cues are less affected by reflections at a ground than at a wall, especially ITDs. More importantly, even though binaural cues differ from the anechoic case, they are not very variable: the ground is generally horizontal, the distance between the ears and the ground is fixed (or at least likely to be known by the animal) and the influence of the nature of the ground is relatively small. As we have seen, the interference frequencies are directly related to the delay between the direct and reflected sounds, and therefore to the polar angle and distance. The amplitude of these interferences depends on the nature of the ground, but their frequency does not. Therefore, interferences contributed by the reflection at the ground are a potential spatial cue. It is known that reverberation contributes to the perception of distance and spaciousness (e.g., Blauert, 1997; Truax, 1999)—in particular, the reverberation time. However, the role of single reflections has not been fully described. Preliminary results show that spatial maps of some neurons are unexpectedly more accurate with a reflection than in free-field, at least in the external nuclei of the inferior colliculus of the gerbil (Maki *et al.*, 2005). We suggest that interferences in binaural cues might provide a cue to distance and/or polar angle.

The main cues for polar angle are thought to be (1) monaural spectral notches introduced by the direction-specific attenuation of particular frequencies by the pinna (Algazi *et al.*, 2001; Blauert, 1997; Musicant and Butler, 1985; Tollin and Yin, 2003; Wightman and Kistler, 1992) and (2) head movements (Blauert, 1997; Thurlow *et al.*, 1967). Spectral notches occur at high frequencies and their frequency is positively correlated with polar angle (Maki and Furukawa, 2005; Tollin and Yin, 2003) while the inverse correlation is seen for the interference frequencies [see Fig. 10(B)]. Therefore, these two cues to polar angle should be essentially independent. The potential role of interferences in polar angle estimation was noticed in a similar study on simulated HRTFs of gerbils with ground reflection (Grace *et al.*, 2008), and is also in agreement with a psychoacoustical study showing that the polar angle of the sound source was estimated with greater accuracy with a sound-reflecting surface on the floor (Guski, 1990). This effect was not seen with a wall reflection, which suggests that the auditory system indeed relies on the knowledge of the head-ground distance to extract the relevant information.

However, interference frequency provides an ambiguous cue to polar angle because it also depends on distance. Distance perception is generally seen as less accurate than for lateral angle and polar angle in mammals (Bronkhorst and Houtgast, 1999; Zahorik *et al.*, 2005). Several cues have been previously investigated [see reviews in Coleman (1963), Mershon and Bowers (1979) and Brown and May (2005)]: (1) level of known sounds: the sound intensity varies with distance according to the inverse-square law; (2) frequency spectrum: high-frequency components of broadband signals are attenuated more rapidly by air propagation than low-frequency ones; (3) movement parallax: the direction of a source is less modified by listener movements for a distant source than for a close source; (4) acoustic field width: it should be larger for a close source; (5) direct-to-reverberant energy ratio: at long distance, the many reflections induced by the propagation of sounds in all directions increase the amount of energy received after the direct sound wave (Bronkhorst and Houtgast, 1999; Mershon and King, 1975; Shinn-Cunningham *et al.*, 2001; Yan-Chen Lu and Cooke, 2010; Zahorik *et al.*, 2005). Many studies on distance perception suggest that auditory image distortion, including reflections and scattering, by natural environments is an important cue for distance perception (Brown and Gomez, 1992; Brown and Waser, 1988; Waser and Brown, 1986; Wiley and Richards, 1978). For instance, it has been shown that distance judgments are more accurate in a reverberant space than in an anechoic space (Mershon and Bowers, 1979; Mershon and King, 1975; Nielsen, 1993; Sheeline, 1982; Zahorik, 2002). In addition to these cues, our results suggest that binaural interferences might be another one. Nevertheless, for sources in the horizontal plane, which is probably the most common situation, interferences occur at high frequencies (>20 kHz) at distances greather than 2 m for guinea pigs [Fig. 10(A)], meaning that only a few interference peaks will fall within the hearing range of the animal. For these species, this cue might therefore be more useful for close sources. For humans, these interferences could provide information over a larger range (for example, the first interference frequency is 76 Hz at 1.5 m, see Table IV). This hypothesis could be tested with psychophysical experiments.

These interferences are also seen in monaural signals, and therefore they could be seen as monaural cues. However, only the binaural cues are independent of the sound source: for example, frequency-dependent changes in level in a monaural signal can be due either to reflections or to the spectrum of the source. If binaural rather than monaural interference cues are used by the auditory system, one prediction is that their effect should only be seen away from the median plane, where ITDs and ILDs are essentially zero.

Whether early reflections come from the ground or from a wall, and even though their impact on binaural cues may depend on many factors, these binaural cues are reproducible and temporally stable. Thus, even if ITDs and ILDs cannot be unambiguously mapped to the location of the sound source, they could still be used as reliable spatial cues to isolate a sound source from a noisy background. Perhaps a person or animal could learn to associate a source with a particular pattern of frequency-dependent ITD and ILD, which could then be used to isolate its signal from those of competing sources, even if this binaural pattern cannot be accurately associated with a particular spatial location. This suggestion has an important implication: the large ITDs and ILDs due to early reflections are not simply "noise" to be filtered, but instead are naturally occurring cues that may be encoded by the auditory system.

E. The natural distribution of binaural cues

When early reflections are considered, the range of ITDs and ILDs is extended, compared to the anechoic case. This observation is most interesting for ITDs. In an anechoic environment, the ITD is limited by the size of the head. For example, in humans, it does not exceed 650–700 μs in high frequencies. In low frequencies, it can be about 50% larger because of diffraction effects (Kuhn, 1977), but it is still limited. However, with an early reflection, we have seen that a discontinuity in IPD occurs at the interference frequency, and this implies that the IPD can be arbitrarily large. This means that the ITD can take any value within the π-limit, i.e., between $-1/(2f)$ and $1/(2f)$, where f is the frequency. In many species, many binaural neurons are tuned to best delays that are greater than the maximum range of ITDs in an anechoic environment (McFadden, 1973). The proportion of such neurons differ between species but it has been consistently observed in rabbit (Kuwada *et al.*, 1987), guinea pig (McAlpine *et al.*, 2001), cat (Hancock and Delgutte, 2004; Kuwada and Yin, 1983; Yin and Chan, 1990), gerbil (Brand *et al.*, 2002), chinchilla (Thornton *et al.*, 2009), kangaroo rat (Crow *et al.*, 1978), chicken (Köppl and Carr, 2008), and barn owl (Wagner *et al.*, 2007). In most of these studies, this proportion is overestimated because the best delays are compared to the maximum ITD measured in high frequencies, which is smaller than the actual range incorporating the diffraction effects in low frequency (compare for example McAlpine, 2005 and Sterbing *et al.*, 2003). However, it remains that a significant number of binaural neurons are tuned to ITDs that lie outside the range of anechoic ITDs. This observation has motivated a new theory of ITD processing in mammals, according to which ITD is represented by the relative activity of two populations with symmetrical best delays lying outside the natural range (Grothe *et al.*, 2010), a strategy sometimes referred to as slope coding or the two-channel model. This theory is in contrast with the "peak coding" theory (Carr and Konishi, 1990), where ITD is represented by the best delay of the maximally activated neuron. Note that other coding strategies are possible (Colburn, 1973). Our results imply that the natural range of ITDs is much larger than expected from anechoic measurements when considering reflections on the ground or on obstacles: it can take any value within the π-limit. Therefore, the large best delays observed in binaural neurons of small mammals are consistent with peak coding, and more importantly they make the two-channel model problematic because the ratio of activities in the two channels is an ambiguous representation of ITD when the best delay lies within the natural range of ITDs, i.e., different ITDs give the same ratio. It could be argued that large ITDs due to reflections are disturbances and therefore there is no reason for the auditory system to encode them. However, as we have seen, for a reflection at the ground, these large ITDs due to reflections contribute information about sound location rather than noise, because they are reproducible cues. For reflections on walls or obstacles, even though these ITDs may not contribute information about sound location, they are still temporally stable and therefore potentially convey spatial information for segregating sound sources. Thus, it does not seem implausible that the auditory system may encode these large ITDs.

In addition, we also note that binaural neurons compare the information only after the physical signals have been processed by the auditory periphery. As has been noted by other authors, such nonlinear processes, including for instance half-wave rectification and adaptation, can cause monaural interactions between direct and reflected sounds that can result in unexpected changes in the cues effectively seen by the binaural neurons (Hartung and Trahiotis, 2001; Trahiotis and Hartung, 2002).

F. Summary

In realistic auditory environments, binaural cues can be modified by reflections. When the delay between the direct and reflected sounds is long, the auditory system can isolate the onset of the direct sound. However, in many cases, these delays are very short. For example, for a reflection at the ground, the delay of the reflected sound is no more than $2p/c$, where p is the distance of the ears from the ground and c is the speed of sound. This gives about 10 ms for humans, about 1 ms for cats and less for smaller mammals. In many practical situations, the delay is substantially lower than this higher limit.

This delay Δ results in destructive interferences at each ear at frequencies about $f = 1/(2\Delta) + n/\Delta$, where n is an integer, which produce large modifications of ITDs and ILDs near these frequencies. Therefore, binaural cues in an ecological environment, even a simple one with only a ground, are not the same as in an anechoic environment. These modifications are larger for ILDs than for ITDs. They are larger for a vertical wall than for a horizontal ground, because the interaural axis is parallel to the ground. In all cases, they remain very significant near interference frequencies. These modifications depend on the delay of the reflected sound, and therefore on source distance. At a finer level of detail, they also depend on the acoustical properties of the reflecting surface. Hard surfaces (e.g., concrete) reflect more energy than soft ones (e.g., snow) and therefore have a stronger impact on binaural cues, but the impact is significant with typical natural surfaces. The analyses also imply that the range of ITDs and ILDs in natural environments is significantly extended compared to the anechoic case.

As a final remark, we note that the ears of small mammals are very close to the ground and possibly to objects on the ground, making their acoustical environment more variable. Thus, their acoustical cues for sound localization may be quite different from those available to humans, with their ears about 1.70 m above the ground. These differences should be kept in mind when extrapolating the results of animal studies to humans, or to other species: binaural cues do not only depend on the shape of the head and ears, but also on the properties of the natural acoustical environment.

ACKNOWLEDGMENTS

This work was supported by the European Research Council (Grant No. ERC StG 240132). We thank the reviewers for their constructive suggestions. We also thank Marc Rébillat for comments on the manuscript.

APPENDIX A: LIST OF SYMBOLS

φ_{S^*}	Incidence angle of the reflected wave on the wall
arg	Argument of a complex number
c	Speed of sound (343 m/s here)
d	Distance source-ears (direct path)
d^*	Distance source-ears (reflection path)
δ	Absolute delay of the direct sound
δ^*	Absolute delay of the reflected sound
D	Delay direct sound—reflection (airhead model)
D_L/D_R	D at the left/right ear, respectively
$\Delta_{\phi R}$	Delay at the right ear between direct and reflected waves due to sound diffraction (s)
erfc	Complementary error function
f_0	First notch frequency in a spectrum (Hz)
f_p	Interference pattern spacing in a spectrum (Hz)
ϕ	Phase shift
φ_{M}	Polar angle for the left ear
φ_S	Polar angle of a point source S
F	"Ground wave" function
H	Head related transfer function (HRTF)
H^{rec}	HRTF after reflection
H_L/H_R	HRTF at the left/right ear, respectively
h_m	m-th order spherical Hankel function
i	Imaginary number: square root of -1
k_i	Wave numbers of the sound field in the i-th media
l	Interaural distance
μ	Normalized frequency
n	Integer
O	Center of the head
OD	Orthodromic distance
p	Distance head-ground or head-wall)
P	Complex pressure
P^{rec}	Complex pressure at the receiver
P_m	m-th order Legendre polynomial
Q	Spherical reflection factor
r	Radius of sphere
R	Plane wave reflection coefficient
ρ	Normalized distance to the source
S	Point source
S'	Mirror source
σ	"Effective" flow resistivity (Pa.s.m-2)
S_L/S_R	Signal at the left/right ear, respectively
τ	Phase delay of Q
θ_{M}	Lateral angle for the left ear
θ_{S}	Lateral angle of a point source S
(X,Y,Z)	Cartesian coordinate system
x_S,y_S,z_S	Cartesian coordinates of S
w	Numerical distance
Z_i	Specific acoustic impedances of the i-th media

APPENDIX B: GEOMETRICAL MODELS OF REFLECTION

We consider the case where a sound wave is reflected at an obstacle before reaching its target. We consider two situations: reflections on a horizontal ground or on a vertical wall, parallel to the median plane (Fig. 2). We give here the detailed calculations for the delay between direct and reflected sounds as a function of the distance from the source to the head and the polar (ground case) or lateral (wall case) angle of the sound source to the head. Following the notation used in Fig. 2, the angles of the reflection relative to the head are given by the following equations, in the case of a reflecting ground:

$$\theta_{S^*} = \theta_S, \tag{B1}$$

$$\varphi_{S^*} = \arctan\left(\frac{d\cos(\varphi_S)}{2p + d\sin(\varphi_S)}\right) - \frac{\pi}{2}, \tag{B2}$$

$$d^* = \frac{d\cos(\varphi_S)}{\cos(\varphi_{S^*})}. \tag{B3}$$

In the case of a reflecting wall, both lateral and polar angles are modified by the reflection. The easiest way to compute angles for S^* is to consider the Cartesian coordinates system (X,Y,Z): in that, S^* is a translation of S along the Y axis (that of the two ears, which is perpendicular to the wall and therefore parallel to SS^*). We have

$$\begin{gathered} x_S = d\cos\varphi_S\cos\theta_S = x_{S^*} = d^*\cos\varphi_{S^*}\cos\theta_{S^*}, \\ y_S = d\cos\varphi_S\sin\theta_S = 2p - y_{S^*} = 2p - d\cos\varphi_{S^*}\sin\theta_{S^*}, \\ z_S = d\sin\varphi_S = z_{S^*} = d^*\sin\varphi_{S^*}, \end{gathered} \tag{B4}$$

which gives

$$\theta_{S^*} = \arctan\left(\frac{2p - d\cos(\varphi_S)\sin(\theta_S)}{d\cos(\varphi_S)\cos(\theta_S)}\right), \tag{B5}$$

$$\begin{aligned} d^* &= \sqrt{x_{S^*}^2 + y_{S^*}^2 + z_{S^*}^2} \\ &= \sqrt{d^2 - 2p \times d\cos(\varphi_S)\sin(\theta_S) + 4p^2}, \end{aligned} \tag{B6}$$

$$\varphi_{S^*} = \arcsin\left(\frac{d\sin(\varphi_S)}{d^*}\right). \tag{B7}$$

These results are used in the geometrical models of reflections described in Sec. II.

APPENDIX C: ACOUSTICAL MODEL OF REFLECTIONS ON NATURAL SURFACES

Here, we give details of a model for the modifications of a sound wave when it is reflected by a natural surface in a realistic outdoor environment. In the following, we describe the ground-reflection model. The equations are identical for the wall-reflection model, with φ_{S^*} replaced by the incidence angle α_{S^*} of the reflected wave on the wall. Note that as the wall being parallel to the (X,Z) median plane (see Appendix B), then if O is the center of the head, α_{S^*} is equal to the angle between OS^* and its projection on the median plane (X,Z). Thus,

$$\begin{aligned} \alpha_{S^*} &= \arccos\left(\frac{\sqrt{x_{S^*}^2 + z_{S^*}^2}}{d^*}\right) = \arccos\left(\frac{\sqrt{d^{*2} - y_{S^*}^2}}{d^*}\right) \\ &= \arccos\left(\sqrt{1 - \cos^2(\varphi_{S^*})\sin^2(\theta_{S^*})}\right). \end{aligned} \tag{C1}$$

As explained in Sec. II B, we use the Weyl–Van der Pol solution (Sutherland and Daigle, 1998) for the boundary conditions of a spherical sound wave reflected on a plane. The complex sound field P^{rec} at the receiver is well approximated by the equation

$$P^{\mathrm{rec}} = P(d,f) + Q(d^*,f,\varphi_{S^*}) \times P(d^*,f), \tag{C2}$$

where Q is the spherical reflection factor and $P(d,f)$ is the sound field amplitude at frequency f and distance d from the source in the absence of reflecting surfaces. In the following, all quantities except angles implicitly depend on frequency. Q can be written as $Q = R + (1-R)F(w)$, where R is the plane wave reflection factor and $(1-R)F(w)$ is a boundary correction. The plane wave reflection coefficient R is (Chessell, 1977; Embleton *et al.*, 1983)

$$R = \frac{\sin\varphi_{S^*} - \dfrac{Z_1}{Z_2}\left(1 - \dfrac{k_1^2}{k_2^2}\cos^2\varphi_{S^*}\right)^{0.5}}{\sin\varphi_{S^*} + \dfrac{Z_1}{Z_2}\left(1 - \dfrac{k_1^2}{k_2^2}\cos^2\varphi_{S^*}\right)^{0.5}}. \tag{C3}$$

Z_1 and Z_2 are the specific acoustic impedances of the air and ground surface, respectively. $F(w)$, also known as the "ground wave" function or as the "boundary loss factor," is equal to

$$F(w) = 1 + i\sqrt{\pi w}e^{-w}\operatorname{erfc}(-i\sqrt{w}), \tag{C4}$$

where

$$w = i\frac{4\pi f d^*}{c(1-R)^2}\left(\frac{Z_1}{Z_2}\right)^2\left(1 - \frac{k_1^2}{k_2^2}\cos^2\varphi_{S^*}\right) \tag{C5}$$

is called the "numerical distance," erfc is the complementary error function, k_1 and k_2 are the wave numbers of the sound field in the air and ground surface, respectively. $F(w)$ describes the interaction of the curved wavefront with a ground of finite impedance. If the wavefront is plane ($d^* \to \infty$) then $|w| \to \infty$ and $F \to 0$ while if the surface is acoustically hard, then $|w| \to 0$ and $F \to 1$ (also $R = 1$), so $Q = 1$. Numerical computation of F is unstable for high values of w and was performed using algorithms in (Weideman, 1994).

The acoustic impedance of a surface (such as Z_1 and Z_2) is the ratio of the amplitude of the sound pressure to the amplitude of the particle velocity of an acoustic wave that impinges on the surface. Both concrete and densely packed glass fiber are high impedance materials relative to air, whereas grass and some foams are low impedance surfaces. If a sound wave changes medium, the ratio of the acoustic impedances of the media Z_2/Z_1 determines the efficiency of the energy transfer.

There have been numerous models estimating k_2/k_1 and Z_2/Z_1 for typical outdoor surfaces. A widely used one, called the Delany–Bazley model (Delany and Bazley, 1970), involves a single parameter, the "effective" flow resistivity σ to characterize the ground. Its units are Pa s m^{-2}. Following time conventions in Embleton *et al.* (1983) and improvements of the Delany–Bazley model by Miki (1990) we have the expressions

$$\frac{Z_2}{Z_1} = 1 + 0.0699\left(\frac{f}{\sigma}\right)^{-0.632} + 0.1071i\left(\frac{f}{\sigma}\right)^{-0.632}, \quad \text{(C6)}$$

$$\frac{k_2}{k_1} = 1 + 0.1093\left(\frac{f}{\sigma}\right)^{-0.618} + 0.1597i\left(\frac{f}{\sigma}\right)^{-0.618}, \quad \text{(C7)}$$

which were considered valid in the range $0.01 < \frac{f}{\sigma} < 1$ originally but which remain well behaved in a larger frequency range. This model may be used for a locally reacting ground as well as an extended reaction surface.

Several tables for flow resistivity σ have been published (see Cox and D'Antonio, 2009). They agree on values around $\sigma = 2.10^4$ for snow, $\sigma = 10^5$ for grass fields or forest floor, and around $\sigma = 6.10^5$ for sand or dirt, a roadside with rocks less than 4 in. in size. σ can reach as much as 3×10^7 for asphalt or 2×10^9 for concrete. In this paper, we chose $\sigma = 10^5$ and $\sigma = 6 \times 10^5$ as moderate values for σ in order to simulate credible outdoor environments encountered by small mammals.

APPENDIX D: SPHERE MODEL

We describe here our model of HRTFs. We use a spherical head model with shifted ears, for which the diffraction function is completely known and has been extensively described, for instance, in (Duda and Martens, 1998; Ono *et al.*, 2008). Briefly, simulated HRTFs can be obtained from the frequency-domain solution for the diffraction of an acoustic wave by a rigid sphere modeling the head.

The source S is at a distance d from a sphere of radius r. Let θ be the angle of incidence between the ray from the center of the sphere to the source and the ray to the measurement point on the surface of the sphere. Given the symmetry axis of a sphere, one angle is enough to define the incidence angle. The transfer function at the surface of the sphere is then given by

$$H(d,f,\theta,r) = -\frac{\rho}{\mu}e^{-i\mu\rho}\sum_{m=0}^{\infty}(2m+1)P_m(\cos\theta)\frac{h_m(\mu\rho)}{h'_m(\mu\rho)}, \quad \text{(D1)}$$

where $\rho = d/r \gg 1$, $\mu = (2\pi r/c)f$, h_m is the m-th-order spherical Hankel function, h'_m its derivative, and P_m is the m-th order Legendre polynomial (Rabinowitz *et al.*, 1993; Rayleigh and Lodge, 1904).

For a spherical head model, $r\theta$ is equal to the shortest distance that the sound wave has to cover to reach the ear, i.e., the shortest distance at the surface of the sphere between an ear of coordinates (θ_M, φ_M) and the incidence angles (θ_S, φ_S) of the sound wave. This is equal to the orthodromic distance $r \times \mathrm{OD}((\theta_S, \varphi_S); (\theta_M, \varphi_M))$ between these two points (see Fig. 7) given by Deza and Deza (2006):

$$\mathrm{OD}((\theta_S, \varphi_S); (\theta_M, \varphi_M)) = \arccos(\cos\varphi_S\cos\varphi_M \times \cos(\theta_M - \theta_S) + \sin\varphi_S\sin\varphi_M) \quad \text{(D2)}$$

(note that when ears are assumed to be antipodal, i.e., $(\theta_M, \varphi_M) = (90°, 0°)$, then $\mathrm{OD}((\theta_S, \varphi_S);\ (90°, 0°)) = \arccos(\cos\varphi_S \sin\theta_S)$). Thus, the HRTF at the left ear can be written $H_L(d,f,\mathrm{OD}((\theta_S, \varphi_S);\ (\theta_M, \varphi_M)), r)$ and that of the right ear is $H_R(d,f,\mathrm{OD}((\theta_S, \varphi_S);\ (-\theta_M, \varphi_M)), r)$ with the previous notations, assuming that ears are symmetrical relative to the medial plane.

For computations made over all spherical positions, a grid of 393 spherical positions evenly distributed around the sphere (between –45 and 90° polar angle) was used and is the same as that found in Behrend *et al.* (2004).

APPENDIX E: ITD AND ILD ESTIMATES

The interaural transfer function (ITF) is typically defined as the ratio of contralateral and ipsilateral HRTFs, which we will adapt here to the ratio of left and right HRTFs for clarity of equations all over the paper since the wall is placed on the side of the left ear, i.e.,

$$\mathrm{ITF}(f, d, (\theta_S, \varphi_S)) = \frac{H_L(f, d, (\theta_S, \varphi_S))}{H_R(f, d, (\theta_S, \varphi_S))}. \quad \text{(E1)}$$

From the ITF, we derive the ILD and interaural phase difference (IPD) as follows:

$$\mathrm{ILD}(f, d, (\theta_S, \varphi_S)) = 20\log_{10}|\mathrm{ITF}(f, d, (\theta_S, \varphi_S))|, \quad \text{(E2)}$$

$$\mathrm{IPD}(f, d, (\theta_S, \varphi_S)) = \arg\Big(\mathrm{ITF}(f, d, (\theta_S, \varphi_S))\Big) \quad \text{(E3)}$$

(where the ILD is in dB). To estimate the ITD of direct and reflected sound waves, we chose a conservative estimate, by choosing the ITD consistent with IPD that is closest to the anechoic ITD.

[1]We thank Michael Akeroyd for his remark about the ellipsoidal locus of reflection locations.

[2]Similar phenomena are seen in crosstalk or active-noise cancellation (e.g., Akeroyd *et al.*, 2007; Bai and Lee, 2006; Elliott and Nelson, 1993). In loudspeaker reproduction, each ear receives the summed signals of both speakers. This is analogous to a reflection problem, where the contralateral speaker is seen as the mirror image of the ipsilateral speaker, with a reflecting surface that is orthogonal to the inter-speaker axis.

[3]Orthodromic is equivalent to a great circle distance in spherical trigonometry, i.e., the shortest distance between two points on the surface of a sphere.

Akeroyd, M. A., Chambers, J., Bullock, D., Palmer, A. R., Summerfield, A. Q., Nelson, P. A., and Gatehouse, S. (**2007**). "The binaural performance of a cross-talk cancellation system with matched or mismatched setup and playback acoustics," J. Acoust. Soc. Am. **121**, 1056–1069.

Algazi, V. R., Avendano, C., and Duda, R. O. (**2001**). "Elevation localization and head-related transfer function analysis at low frequencies," J. Acoust. Soc. Am. **109**, 1110–1122.

Bai, M. R., and Lee, C.-C. (**2006**). "Objective and subjective analysis of effects of listening angle on crosstalk cancellation in spatial sound reproduction," J. Acoust. Soc. Am. **120**, 1976–1989.

Behrend, O., Dickson, B., Clarke, E., Jin, C., and Carlile, S. (**2004**). "Neural responses to free field and virtual acoustic stimulation in the inferior colliculus of the guinea pig," J. Neurophysiol. **92**, 3014–3029.

Blauert, J. (**1997**). "Spatial hearing with multiple sound sources and in enclosed spaces," in *Spatial Hearing: The Psychophysics of Human Sound Localization* (MIT Press, Cambridge, MA), pp. 201–286.

Brand, A., Behrend, O., Marquardt, T., McAlpine, D., and Grothe, B. (**2002**). "Precise inhibition is essential for microsecond interaural time difference coding," Nature **417**, 543–547.

Bronkhorst, A. W., and Houtgast, T. (**1999**). "Auditory distance perception in rooms," Nature **397**, 517–520.

Brown, C. H., and Gomez, R. (**1992**). "Functional design features in primate vocal signals: The acoustic habitat and sound distortion," in *Topics of Primatology*, edited by T. Nishida, W. C. McGrew, and P. Marler (Tokyo University Press, Tokyo), pp. 177–198.

Brown, C. H., and May, B. J. (**2005**). "Comparative mammalian sound localization," in *Sound Source Localization*, edited by A. N. Popper and R. R. Fay (Springer, New York), pp. 124–178.

Brown, C. H., and Waser, P. M. (**1988**). "Environmental influences on the structure of primate vocalizations," in *Primate Vocal Communication*, edited by D. Todt, P. Goedeking, and D. Symmes (Springer-Verlag, Berlin), pp. 51–66.

Carr, C., and Konishi, M. (**1990**). "A circuit for detection of interaural time differences in the brain stem of the barn owl," J. Neurosci. **10**, 3227–3246.

Chessell, C. I. (**1977**). "Propagation of noise along a finite impedance boundary," J. Acoust. Soc. Am. **62**, 825.

Colburn, H. S. (**1973**). "Theory of binaural interaction based on auditory-nerve data. I. General strategy and preliminary results on interaural discrimination," J. Acoust. Soc. Am. **54**, 1458–1470.

Coleman, P. D. (**1963**). "An analysis of cues to auditory depth perception in free space," Psychol. Bull. **60**, 302–315.

Cox, T., and D'Antonio, P. (**2009**). "Measurement of absorber properties," in *Acoustic Absorbers and Diffusers: Theory, Design and Application* (Taylor & Francis, New-York), pp. 70–107.

Cranford, J. L. (**1982**). "Localization of paired sound sources in cats: effects of variable arrival times," J. Acoust. Soc. Am. **72**, 1309–1311.

Croghan, N. B. H., and Grantham, D. W. (**2010**). "Binaural interference in the free field," J. Acoust. Soc. Am. **127**, 3085–3091.

Crow, G., Rupert, A. L., and Moushegian, G. (**1978**). "Phase locking in monaural and binaural medullary neurons: implications for binaural phenomena," J. Acoust. Soc. Am. **64**, 493–501.

Delany, M. E., and Bazley, E. N. (**1970**). "Acoustical properties of fibrous absorbent materials," Appl. Acoust. **3**, 105–116.

Dent, M. L., and Dooling, R. J. (**2004**). "The precedence effect in three species of birds (*Melopsittacus undulatus, Serinus canaria*, and *Taeniopygia guttata*)," J. Comp. Psychol. **118**, 325–331.

Dent, M. L., Tollin, D. J., and Yin, T. C. T. (**2009**). "Influence of sound source location on the behavior and physiology of the precedence effect in cats," J. Neurophysiol. **102**, 724–734.

Devore, S., and Delgutte, B. (**2010**). "Effects of reverberation on the directional sensitivity of auditory neurons across the tonotopic axis: Influences of interaural time and level differences," J. Neurosci. **30**, 7826–7837.

Deza, E., and Deza, M. (**2006**). "Geometry and distances," in *Dictionary of Distances* (Elsevier, Amsterdam), pp. 62–133.

Dizon, R. M., and Colburn, H. S. (**2006**). "The influence of spectral, temporal, and interaural stimulus variations on the precedence effect," J. Acoust. Soc. Am. **119**, 2947–2964.

Duda, R. O., and Martens, W. L. (**1998**). "Range dependence of the response of a spherical head model," J. Acoust. Soc. Am. **104**, 3048–3058.

Elliott, S. J., and Nelson, P. A. (**1993**). "Active noise control," IEEE Sign. Process. Mag. **10**, 12–35.

Embleton, T. F. W., Piercy, J. E., and Daigle, G. A. (**1983**). "Effective flow resistivity of ground surfaces determined by acoustical measurements," J. Acoust. Soc. Am. **74**, 1239–1244.

Freyman, R. L., Balakrishnan, U., and Helfer, K. S. (**2001**). "Spatial release from informational masking in speech recognition," J. Acoust. Soc. Am. **109**, 2112–2122.

Giguère, C., and Abel, S. M. (**1993**). "Sound localization: effects of reverberation time, speaker array, stimulus frequency, and stimulus rise/decay," J. Acoust. Soc. Am. **94**, 769–776.

Grace, S. M., Quaranta, E., Shinn-cunningham, B. G., and Voigt, H. F. (**2008**). "Simulation of the binaural environmental transfer function for gerbils using a boundary element method," Acta Acust. Acust. **94**, 310–320.

Griffin, S. J., Bernstein, L. R., Ingham, N. J., and McAlpine, D. (**2005**). "Neural sensitivity to interaural envelope delays in the inferior colliculus of the Guinea Pig," J. Neurophysiol. **93**, 3463–3478.

Grothe, B., Pecka, M., and McAlpine, D. (**2010**). "Mechanisms of sound localization in mammals," Physiol. Rev. **90**, 983–1012.

Guski, R. (**1990**). "Auditory localization: effects of reflecting surfaces," Perception **19**, 819–830.

Hancock, K. E., and Delgutte, B. (**2004**). "A physiologically based model of interaural time difference discrimination," J. Neurosci. **24**, 7110–7117.

Hartmann, W. M. (**1983**). "Localization of sound in rooms," J. Acoust. Soc. Am. **74**, 1380–1391.

Hartmann, W. M., and Rakerd, B. (**1989**). "Localization of sound in rooms. IV. The Franssen effect," J. Acoust. Soc. Am. **86**, 1366–1373.

Hartung, K., and Trahiotis, C. (**2001**). "Peripheral auditory processing and investigations of the 'precedence effect' which utilize successive transient stimuli," J. Acoust. Soc. Am. **110**, 1505–1513.

ISO (**1993**). 9613–1:1993, *Acoustics—Attenuation of Sound During Propagation Outdoors—Part 1: Calculation of the Absorption of Sound by the Atmosphere* (International Organization for Standardization, Geneva).

Joris, P. X. (**2003**). "Interaural time sensitivity dominated by cochlea-induced envelope patterns," J. Neurosci. **23**, 6345–6350.

Joris, P., and Yin, T. C. T. (**2007**). "A matter of time: Internal delays in binaural processing," Trends Neurosci. **30**, 70–78.

Keller, C. H., and Takahashi, T. T. (**1996a**). "Responses to simulated echoes by neurons in the barn owl's auditory space map," J. Comp. Physiol., A **178**, 499–512.

Keller, C. H., and Takahashi, T. T. (**1996b**). "Binaural cross-correlation predicts the responses of neurons in the owl's auditory space map under conditions simulating summing localization," J. Neurosci. **16**, 4300–4309.

Keller, C. H., and Takahashi, T. T. (**2005**). "Localization and identification of concurrent sounds in the owl's auditory space map," J. Neurosci. **25**, 10446–10461.

Kelly, J. B. (**1974**). "Localization of paired sound sources in the rat: Small time differences," J. Acoust. Soc. Am. **55**, 1277–1284.

Kirikae, I., Nakamura, K., Sato, T., and Shitara, T. (**1971**). "A study of binaural interaction," Ann. Bulletin No. 5, Research Institute of Logopedics-Phoniatrics, University of Tokyo, pp. 115–126.

Köppl, C., and Carr, C. (**2008**). "Maps of interaural time difference in the chicken's brainstem nucleus laminaris," Biol. Cybern. **98**, 541–559.

Kuhn, G. F. (**1977**). "Model for the interaural time differences in the azimuthal plane," J. Acoust. Soc. Am. **62**, 157–167.

Kuwada, S., Stanford, T. R., and Batra, R. (**1987**). "Interaural phase-sensitive units in the inferior colliculus of the unanesthetized rabbit: Effects of changing frequency," J. Neurophysiol. **57**, 1338–1360.

Kuwada, S., and Yin, T. C. (**1983**). "Binaural interaction in low-frequency neurons in inferior colliculus of the cat. I. Effects of long interaural delays, intensity, and repetition rate on interaural delay function," J. Neurophysiol. **50**, 981–999.

Leakey, D. M. (**1959**). "Some measurements on the effects of interchannel intensity and time differences in two channel sound systems," J. Acoust. Soc. Am. **31**, 977–986.

Litovsky, R. Y., Colburn, H. S., Yost, W. A., and Guzman, S. J. (**1999**). "The precedence effect," J. Acoust. Soc. Am. **106**, 1633–1654.

Lochner, J. P. A., and Burger, J. F. (**1964**). "The influence of reflections on auditorium acoustics," J. Sound Vib. **1**, 426–454.

Maki, K., and Furukawa, S. (**2005**). "Acoustical cues for sound localization by the Mongolian gerbil, *Meriones unguiculatus*," J. Acoust. Soc. Am. **118**, 872–886.

Maki, K., Furukawa, S., and Hirahara, T. (**2003**). "Acoustical cues for sound localization by gerbils in an ecologically realistic environment," presented at the Association for Research in Otolaryngology, Vol. Abst. 26, p. 89.

Maki, K., Furukawa, S., and Hirahara, T. (**2005**). "The effects of sounds reflected from the ground on the spatial response fields of neurons in the gerbil inferior colliculus," presented at the Association for Research in Otolaryngology (New Orleans, LA) , Vol. **28**, pp. 38–39.

McAlpine, D. (**2005**). “Creating a sense of auditory space,” J. Physiol. (London) **566**, 21–28.

McAlpine, D., Jiang, D., and Palmer, A. R. (**2001**). “A neural code for low-frequency sound localization in mammals,” Nat. Neurosci. **4**, 396–401.

McFadden, D. (**1973**). “Letter: Precedence effects and auditory cells with long characteristic delays,” J. Acoust. Soc. Am. **54**, 528–530.

Mershon, D. H., and Bowers, J. N. (**1979**). “Absolute and relative cues for the auditory perception of egocentric distance,” Perception **8**, 311–322.

Mershon, D. H., and King, L. E. (**1975**). “Intensity and reverberation as factors in the auditory perception of egocentric distance,” Percept. Psychophys. **18**, 409–415.

Mickey, B. J., and Middlebrooks, J. C. (**2001**). “Responses of auditory cortical neurons to pairs of sounds: Correlates of fusion and localization,” J. Neurophysiol. **86**, 1333–1350.

Miki, Y. (**1990**). “Acoustical properties of porous materials—Modifications of Delany-Bazley models,” J. Acoust. Soc. Jpn. (E) **11**, 19–24.

Musicant, A. D., and Butler, R. A. (**1985**). “Influence of monaural spectral cues on binaural localization,” J. Acoust. Soc. Am. **77**, 202–208.

Nelson, B. S., and Takahashi, T. T. (**2010**). “Spatial hearing in echoic environments: The role of the envelope in owls,” Neuron **67**, 643–655.

Nielsen, S. H. (**1993**). “Auditory distance perception in different rooms,” J. Audio Eng. Soc. **41**, 755–770.

Ono, N., Fukamachi, S., and Sagayama, S. (**2008**). “Sound source localization with front-back judgement by two microphones asymmetrically mounted on a sphere,” J. Multimedia **3**, 1–9.

Populin, L. C., and Yin, T. C. (**1998**). “Behavioral studies of sound localization in the cat,” J. Neurosci. **18**, 2147–2160.

Rabinowitz, W. M., Maxwell, J., Shao, Y., and Wei, M. (**1993**). “Sound localization cues for a magnified head—Implications from sound diffraction about a rigid sphere,” Presence Teleoperators Virtual Environ. **2**, 125–129.

Rakerd, B., and Hartmann, W. M. (**1985**). “Localization of sound in rooms. II. The effects of a single reflecting surface,” J. Acoust. Soc. Am. **78**, 524–533.

Rakerd, B., and Hartmann, W. M. (**2005**). “Localization of noise in a reverberant environment,” in *Auditory Signal Processing: Physiology, Psychoacoustics, and Models*, edited by D. Pressnitzer, A. Cheveigné, S. McAdams, and L. Collet (Springer-Verlag, New York), pp. 348–354.

Rasmussen, K. B. (**1981**). “Sound propagation over grass covered ground,” J. Sound Vib. **78**, 247–255.

Rayleigh, Lord, and Lodge, A. (**1904**). “On the acoustic shadow of a sphere with an appendix, giving the values of Legendre’s functions from P0 to P20 at intervals of 5 degrees,” Philos. Trans. R. Soc. London, Ser. A **203**, 87–110.

Sheeline, C. (**1982**). *An Investigation of the Effects of Direct and Reverberant Signal Interactions on Auditory Distance Perception*, Ph.D. thesis, Standford Univeristy, pp. 63–70.

Shinn-Cunningham, B., Desloge, J. G., and Kopco, N. (**2001**). “Empirical and modeled acoustic transfer functions in a simple room: Effects of distance and direction,” in IEEE Workshop On Applications Of Signal Processing To Audio And Acoustics 2001, pp. 183–186.

Shinn-Cunningham, B. G., Kopco, N., and Martin, T. J. (**2005**). “Localizing nearby sound sources in a classroom: Binaural room impulse responses,” J. Acoust. Soc. Am. **117**, 3100–3115.

Shinn-Cunningham, B. G., Zurek, P. M., and Durlach, N. I. (**1993**). “Adjustment and discrimination measurements of the precedence effect,” J. Acoust. Soc. Am. **93**, 2923–2932.

Spitzer, M. W., and Takahashi, T. T. (**2006**). “Sound localization by barn owls in a simulated echoic environment,” J. Neurophysiol. **95**, 3571–3584.

Sterbing, S. J., Hartung, K., and Hoffmann, K.-P. (**2003**). “Spatial tuning to virtual sounds in the inferior colliculus of the Guinea Pig,” J. Neurophysiol. **90**, 2648–2659.

Sutherland, L. C., and Daigle, G. A. (**1998**). “Atmospheric sound propagation,” in *Handbook Of Acoustics*, edited by M. J. Crocker (Wiley-IEEE, New York), pp. 305–330.

Thornton, J. L., Koka, K., Jones, H. G., and Tollin, D. J. (**2009**). “A frequency-dependence in both the acoustic interaural time difference cues to sound location and their encoding by neurons in the inferior colliculus,” presented at the ARO, Abstract 529.

Thurlow, W. R., Mangels, J. W., and Runge, P. S. (**1967**). “Head movements during sound localization,” J. Acoust. Soc. Am. **42**, 489–493.

Tollin, D. J., and Yin, T. C. (**2003**). “Spectral cues explain illusory elevation effects with stereo sounds in cats,” J. Neurophysiol. **90**, 525–530.

Trahiotis, C., and Hartung, K. (**2002**). “Peripheral auditory processing, the precedence effect and responses of single units in the inferior colliculus,” Hear. Res. **168**, 55–59.

Truax, B. (**1999**). *Handbook for Acoustic Ecology*, 2nd ed, Compact Disc (Cambridge Street Publishing, Cambridge).

Wagner, H., Asadollahi, A., Bremen, P., Endler, F., Vonderschen, K., and von Campenhausen, M. (**2007**). “Distribution of interaural time difference in the barn owl’s inferior colliculus in the low- and high-frequency ranges,” J. Neurosci. **27**, 4191–4200.

Wallach, H., Newman, E. B., and Rosenzweig, M. R. (**1949**). “The precedence effect in sound localization,” Am. J. Psychol. **62**, 315–336.

Waser, P. M., and Brown, C. H. (**1986**). “Habitat acoustics and primate communication,” Am. J. Primatol. **10**, 135–154.

Weideman, J. A. C. (**1994**). “Computation of the Complex Error Function,” SIAM J. Numer. Anal. **31**, 1497–1518.

Wendt, K. (**1963**). “Das Richtungshören bei der Überlagerung zweier Schallfelder bei Intensitäts- und Laufzeitstereophonie” (“Directional hearing with two superimposed sound fields in intensity- and delay-difference stereophony”), Ph.D. thesis, Rheinisch-Westfälische Technische Hochschule, Aachen, pp. 1–107.

Wightman, F. L., and Kistler, D. J. (**1992**). “The dominant role of low-frequency interaural time differences in sound localization,” J. Acoust. Soc. Am. **91**, 1648–1661.

Wiley, R. H., and Richards, D. G. (**1978**). “Physical constraints on acoustic communication in the atmosphere: Implications for the evolution of animal vocalizations,” Behav. Ecol. Sociobiol. **3**, 69–94.

Wyttenbach, R. A., and Hoy, R. R. (**1993**). “Demonstration of the precedence effect in an insect,” J. Acoust. Soc. Am. **94**, 777–784.

Xiao, X., and Grantham, D. W. (**1997**). “The effect of a free-field auditory target’s motion on its detectability in the horizontal plane,” J. Acoust. Soc. Am. **102**, 1907–1910.

Yan-Chen Lu, and Cooke, M. (**2010**). “Binaural estimation of sound source distance via the direct-to-reverberant energy ratio for static and moving sources,” IEEE Trans. Audio Speech Lang. Process. **18**, 1793–1805.

Yin, T. C. (**1994**). “Physiological correlates of the precedence effect and summing localization in the inferior colliculus of the cat,” J. Neurosci. **14**, 5170–5186.

Yin, T. C., and Chan, J. C. (**1990**). “Interaural time sensitivity in medial superior olive of cat,” J. Neurophysiol. **64**, 465–488.

Zahorik, P. (**2002**). “Assessing auditory distance perception using virtual acoustics,” J. Acoust. Soc. Am. **111**, 1832.

Zahorik, P., Brungart, D. S., and Bronkhorst, A. W. (**2005**). “Auditory distance perception in humans: A summary of past and present research,” Acta Acust. Acust. **91**, 409–420.

Zurek, P. M. (**1987**). “The precedence effect,” in *Directional Hearing*, edited by W. A. Yost and G. Gourevitch (Springer-Verlag, New York), pp. 85–106.